GEOLOGICAL AND GEOPHYSICAL STUDIES OF THE CANTON TROUGH

A THESIS SUBMITTED TO THE GRADUATE DIVISION OF THE UNIVERSITY OF HAWAII IN PARTIAL FULFILLMENT OF THE REQUIREMENTS FOR THE DEGREE OF

MASTER OF SCIENCE

IN GEOLOGY-GEOPHYSICS

MAY 1972

By

Bruce R. Rosendahl

Thesis Committee:

Ralph M. Moberly, Chairman
Gordon A. Macdonald
George H. Sutton
John C. Rose
Herbert H. Veeh

We certify that we have read this thesis and that in our opinion it is satisfactory in scope and quality as a thesis for the degree of Master of Science in Geology-Geophysics.

THESIS COMMITTEE

Chairman

John C. Rose

Gordon A. Macdonald

George H. Sutton

H. Herbert Vaughan

ACKNOWLEDGMENTS

Many persons have been instrumental during the course of this study. I thank Dr. Alexander Malahoff for initiating the R/V MAHI survey and providing helpful suggestions during the formulation of this work. I also thank Dr. Loren Kroenke and A. John Halunen for their valuable assistance throughout this study. Dr. Charles Fein, William C. Burnett and J. Frisbee Campbell have provided guidance in the preparation of this manuscript.

The chemical analyses used in this study were furnished by William C. Burnett and Dr. Charles Fein. Technical assistance in the preparation of this manuscript was provided by Ethel McAfee. Financial support for this study was provided by ONR contract N00014-70-A-0016-0001.

ABSTRACT

Bathymetric, seismic reflection, gravity, magnetic, and petrologic studies have been made of a zone of ridges and troughs in the Central Pacific Basin. This zone extends for at least 500 km east-northeast of the Phoenix Islands and its width may exceed 200 kilometers. Structurally, the zone is divided into a central, northern, and southern province. Within the central province, en échelon volcanic ridges flank an extremely linear, flat-floored trough (the Canton Trough), which locally exceeds 8000 m in depth. Crustal models, constructed from gravity data, indicate crustal thickening and intrusion within this province. Rocks dredged from near the base of the Canton Trough include quartz diorites, diorites, gabbros, diabases, altered basalts, greenstones, and relatively fresh volcanic cinder and glass. Whereas extensive block-faulting characterizes the northern province, deformation within the southern province is restricted to its northern edge. The Canton Trough zone may be the extension of the Clipperton fracture zone into the Central Pacific Basin, and, as such, it may have been formed by a reorientation of spreading centers along the East Pacific Rise during the Cretaceous period. However, rejuvenation must be involved to account for unaltered igneous rocks and faulted sediments. Magnetic lineations, if unrelated to structure, are not easily reconciled with this model, since they trend E-NE, oblique to the structure. If these lineations prove

to be sea-floor spreading anomalies, the reorientation-rejuvenation model would not be a tenable hypothesis for the Canton Trough zone.

TABLE OF CONTENTS

LIST OF TABLES

LIST OF FIGURES

INTRODUCTION

A. Purpose and scope

During the summer of 1970, a research team from the Hawaii Institute of Geophysics aboard the R/V MAHI conducted a geophysical survey of a small region of the Central Pacific Basin. We had the foreknowledge that an extremely deep trough lay within this region and we were therefore able to concentrate our survey over the feature. The trough and its immediate extension was subsequently named the Canton Trough [Halunen et al., 1970] because the trend of the feature is toward Canton Island, the nearest land.

Early during the survey it was recognized that the trough's topographic relief was indeed remarkable and that its depths were the greatest recorded for any mid-ocean deep. On these observations alone, the region merited additional study. Moreover, from preliminary examination of the survey data [Halunen et al., 1970; Rosendahl and Halunen, 1971], it became readily apparent that the region would prove to be especially significant from the standpoint of mid-ocean tectonics. This present study was initiated primarily to deduce, from the geological and geophysical observations, the tectonic processes responsible for the formation of the Canton Trough.

Because the ultimate goal of this work is tectonic interpretation, the analyses of all available data are

requisite. These data analyses are presented here as follows: bathymetry; seismic reflection profiling; gravity; magnetics; and petrology and geochemistry. Tectonic processes are discussed in the final part of this work.

B. Geologic setting

Menard [1964, 1967] was the first to report that troughs and ridges were present in isolated areas of the Central Pacific Basin. One of these areas, located northeast of the Phoenix Islands, contains the extremely deep trough over which the R/V MAHI survey was made. This region is located within the south-central part of the Basin, encompassing the area between about 166°W and 172°W and extending from the Equator to 3° 30'S (Figure 1). Engel and Engel [1970], in describing rocks dredged from a very deep trough in the Pacific, termed it the "Argo Trench." Although there is some confusion as to its location, it is likely that the feature is part of the Canton Trough discussed herein.

Kroenke et al. [1971] have deemed the Central Pacific Basin sufficiently distinctive in its physiography, structure, and stratigraphy to be considered a submarine geological province. The province is bordered on the north by the Mid-Pacific Mountains [Hamilton, 1956] and on the south by the Manahiki Plateau [Heezen et al., 1966]. On the east lie the Line Islands, and on the west the Radak, Gilbert and

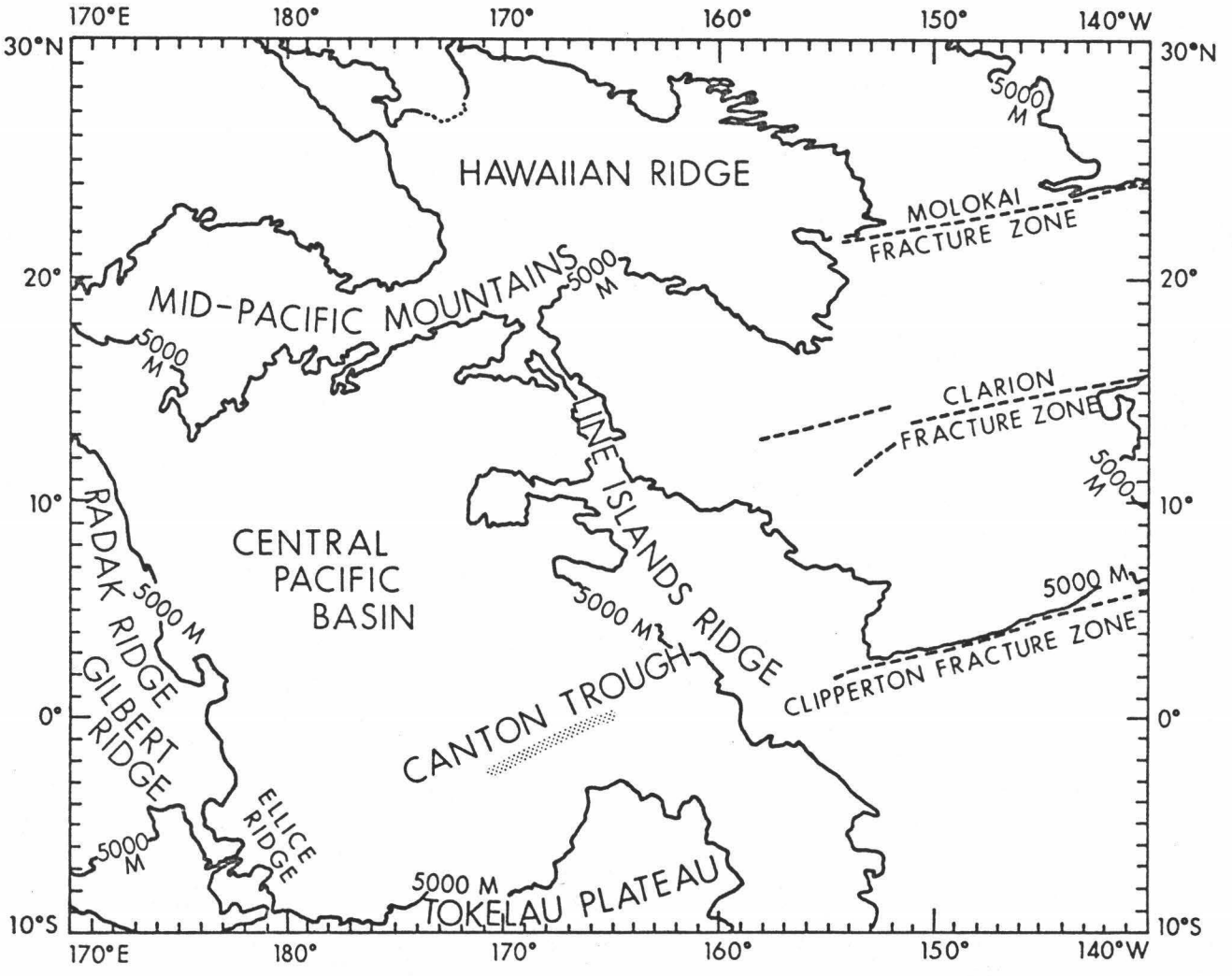

Fig. 1. Location map. Regional 5000-m contour (from unpublished HIG chart) outlines submarine geological provinces [Kroenke et al., 1971].

Ellice ridges. Characteristically, the basin is deeper than 5000 m, rather uncomplicated with respect to "acoustic layering" as deduced by seismic reflection profiling, and dotted with numerous abyssal hills [Kroenke, 1970]. Tectonically the basin is aseismic and acts as part of the Pacific plate. Some of the great East Pacific fracture zones, particularly the Clarion and Clipperton, and possibly the Galapagos and Marquesas, may extend into the region. The relationship of the Canton Trough to the Clipperton fracture zone forms an integral part of this study.

BATHYMETRY

A. General

Bathymetric data were obtained from 3.5 and 12 kHz echo-sounding systems along virtually all traverses shown in Figure 2. Traverses are relatively close-spaced between about 167°W and 169° 30'W, and bathymetric control is considered excellent, but control east of 167° and west of 169° 30' is poor. Near the Phoenix Islands, soundings from Oceanographic Office Chart 0124 supplement the data that were used to construct the bathymetric contour map shown in Figure 3. This map, contoured at intervals of 200 m, is based upon an assumed uniform velocity of 1500 m/sec for sound in sea water.

Bathymetric profiles, as such, are not presented since the seismic reflection profile tracings shown in Figure 5 adequately serve the purpose. Although these tracings will be discussed in detail in the part on seismic reflection in this study, they are referred to in the following discussion.

B. Description

The Canton Trough region is apparently a zone of nearly parallel, elongate ridges and troughs that strike N69°E. This remarkable linearity exceeds 500 km, extending eastward beyond the surveyed region (Figures 3 and 4). Individual topographic features are discontinuous throughout the area

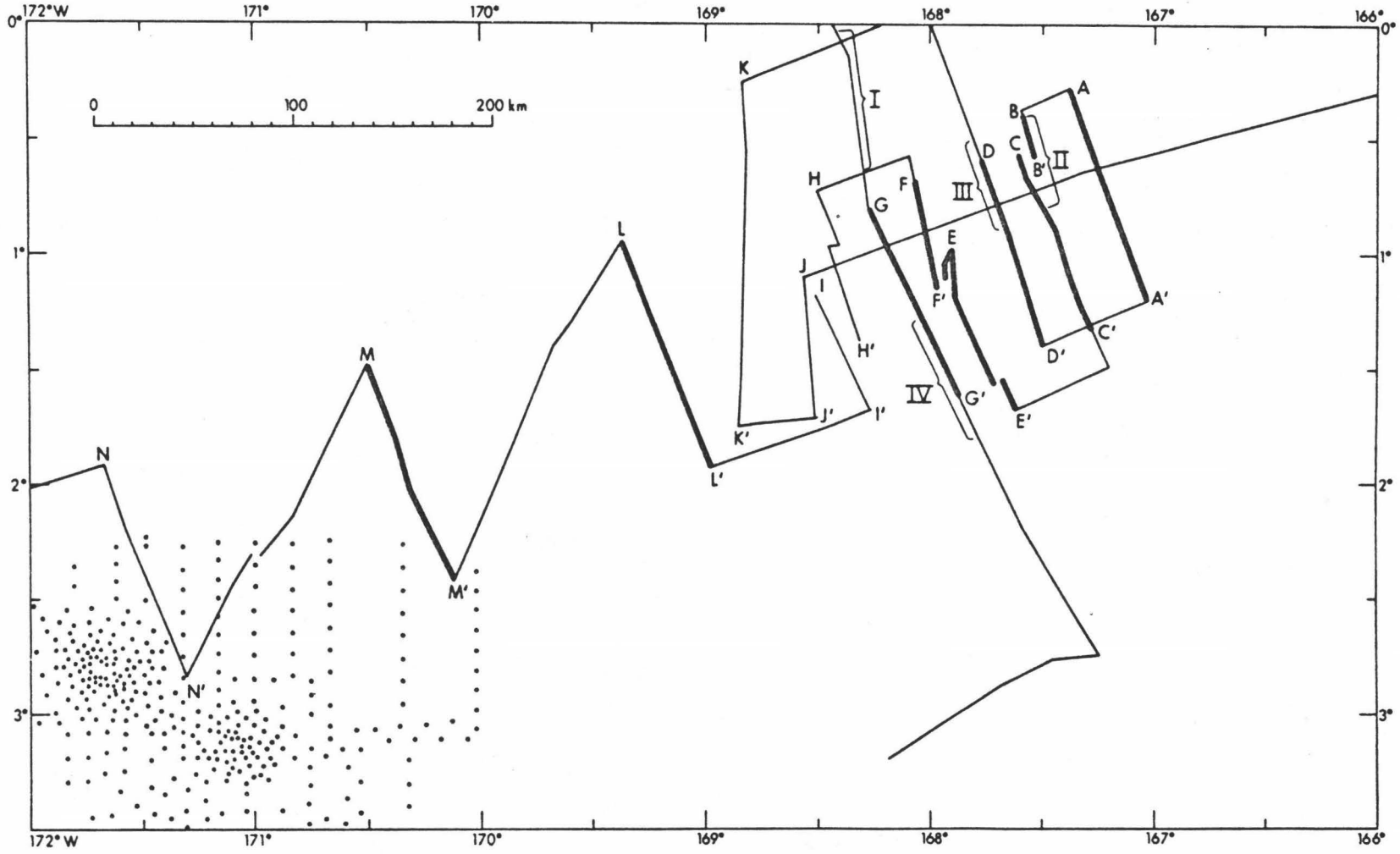

Fig. 2. R/V MAHI ship tracks. Heavy-lined traverses indicate location of reflection profile tracings shown in Figure 5. Roman numerals indicate location of reflection records shown in Figure 6. Solid dots indicate location of soundings from Oceanographic Office chart 0124.

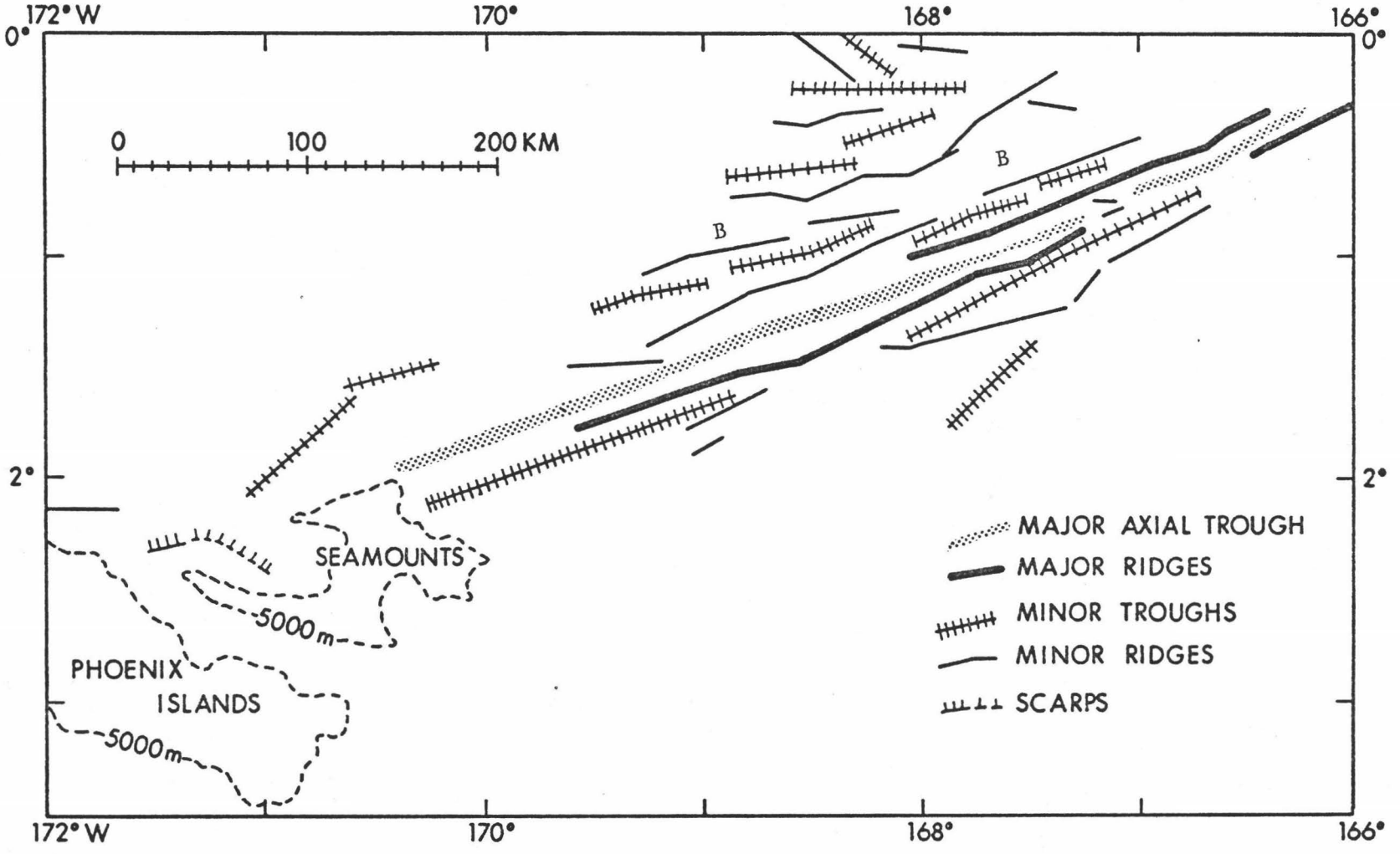

Fig. 4. Bathymetric lineations. Location of northern turbidite basin designated by letter B.

shown in Figures 3 and 4, although some can be traced for considerable distances.

The most outstanding features are the axial trough and its bordering ridges. The axial trough can be traced from 167° 15'W to about 170° 20'W (from profile CC' through profile MM' in Figure 5). The trough is not present as a distinct feature in profile AA', but it reappears to the east as a poorly defined 6400 m deep. West of 170° 20'W the trough is not observed. The distance over which the trough is continuous exceeds 380 km, yet the feature is never wider than 15 km and often less than 10 kilometers. Maximum depths slightly exceed 8000 m (corrected according to Matthew's tables) along profile FF', and are greater than 7800 m for about 85 km between profile EE' and traverse HH'. Depths such as these are only found elsewhere within the major trenches bordering the Pacific. The floor of the trough is everywhere flat and only locally contains much sediment.

The axial deep is usually bordered by either one or two ridges, which are less continuous than the trough. A northern ridge is apparent from about 166° 10'W through 168°W. The major peak shown in profile AA' is probably the northern ridge seen in profiles CC' and DD', for which a minimum depth of about 3200 m was recorded between 166° 30'W and 167°W. The southern ridge can be seen near the extreme right margin of Figures 3 and 4, and appears in profiles BB'

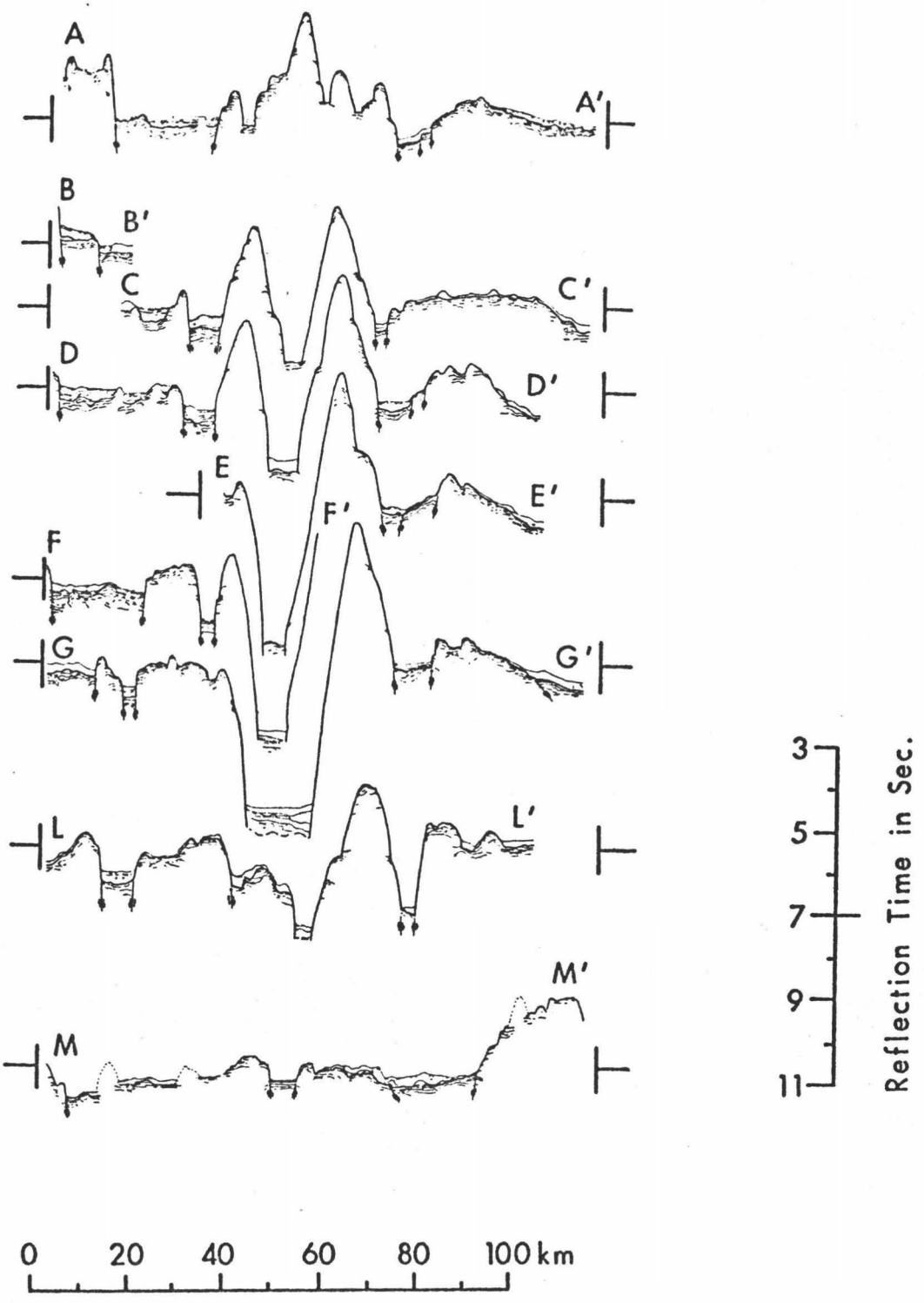

Fig. 5. Seismic reflection profile tracings aligned along axial trough and major ridges. Location of tracings shown in Figure 2. Vertical exaggeration about 10 x.

through LL' in Figure 5. It is not distinct in profile AA' or west of profile LL'. Wherever the southern and northern ridges are both present, the southern ridge is the more prominent. Maximum relief between the southern ridge and axial deep occurs along profile GG' and traverse HH'. Peak-to-trough relief here approaches 5100 m in horizontal distances of less than 17 kilometers. Within this region ridge slopes are locally as great as 28° and generally greater than 20°. It should be noted here that the maximum morphological development of the trough and the southern ridge is nearly coincident, and apparently at the expense of the northern ridge, as discussed in the following sections of this work.

On either side of the ridge-trough system, bathymetric features appear generally less continuous and linear and more subdued, at least partly the result of poorer control. A relatively wide, flat basin is situated on the northern side of the system between 167°W and 169°W. This feature, labeled B in Figure 4, appears in profiles AA' through GG' and is shown in photographs II and III in Figure 6. North of this feature, the topography is a series of troughs and ridges like that shown in photograph I, Figure 6. South of the ridge-trough system, a rather gentle arch-like feature can be seen extending from profile AA' through profile GG'. In profiles west of GG' it is indistinct or absent. The region south of the arch is relatively flat for at least

Fig. 6. Reproductions of selected seismic reflection profiles. Vertical exaggeration about 10 x.

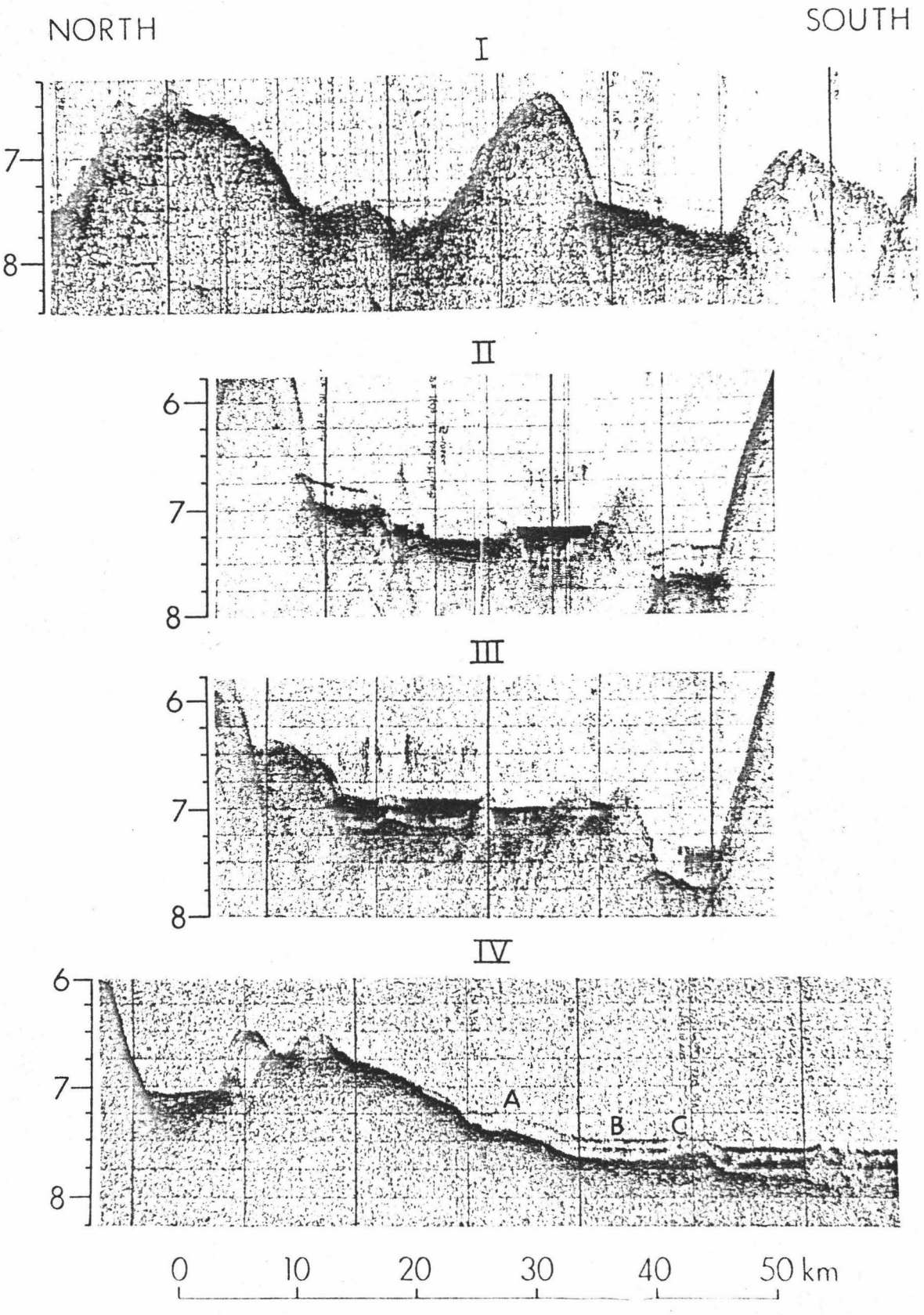
NORTH
SOUTH
I
7
8
II
6
7
8
III
6
7
8
IV
6
7
8
A
B
C
0
10
20
30
40
50 km

75 km along GG'. The southwestern end of the Canton Trough region is characterized by seamounts and islands.

SEISMIC REFLECTION STUDIES

A. General

During the R/V MAHI survey of the Canton Trough, continuous seismic reflection profiling was conducted along the ship tracks shown in Figure 2. The heavy-lined, lettered traverses in this figure correspond to profile tracings shown in Figure 5. The segments labeled with roman numerals show the location of the photographic reproductions of reflection records presented in Figure 6. The tracings in Figure 5 are aligned with respect to the axial deep and the adjacent ridges.

The reflection profiling technique here involved the use of dual sound sources: a 5000-joule sparker and 40-cubic-inch air gun. Incoming signals, received on a linear array of hydrophones, were filtered to the desired frequencies and recorded on several wet-paper-type recorders. The general technique has been described by many workers, including Hersey [1963] and Ewing and Ewing [1970]. An excellent summary is provided by Moore [1969] and need not be repeated here. A detailed description of the method used aboard the R/V MAHI is given elsewhere [Kroenke, ms. submitted to Geol. Soc. Amer.].

B. Seismic reflection profile tracings

Profile tracings are employed in this study as a means of simplifying the original reflection records, while retaining their structural significance. In effect, the tracings are an attempt to remove unwanted marks resulting from noise, multiples, double pulses, and hyperbolic reflections. Of these, hyperbolic reflections posed the greatest difficulty. Within the Canton Trough region, hyperbolic traces are caused by point reflections from features not directly beneath the ship (side echoes) and from topographic highs. Their complete removal involves the use either of tedious geometrical constructions or of mathematical analyses for given point reflectors [Krause, 1962; Krause et al., 1964]. In this study, templates were constructed which approximated hyperbolic phenomena produced by point sources and allowed slope corrections to be applied to major topographic features. The precision depth records produced by the 12 kHz echo-sounding system were also valuable for this purpose because they show more closely the true slope of topographic features. It is believed that the reflection profile tracings in Figure 5 for the most part show only real reflectors.

The use of reflection tracings in the interpretation of structure and lithology is hampered by several factors. First, it is practically impossible to remove completely the previously discussed unwanted marks, and even with corrections

the attitude of any reflecting surface cannot be precisely determined. Second, there are limitations to the resolution capabilities of the profiling system. To obtain reasonably good resolution and penetration, seismic reflection profiles were normally recorded for two frequency bands, 50-100 Hz (low) and 150-300 Hz (high). On a third recorder, these bands are combined to form a mixed-frequency record. In the construction of profile tracings, the low-frequency records were used for delineation of deeper reflectors, while the higher frequency records, in conjunction with 3.5 kHz records, were used for the resolution of closer spaced, shallower reflectors. Even with the higher frequency band, however, the practical maximum resolution is about 2 meters. Since this value is larger than the thicknesses of many sedimentary beds, reflectors traced probably often represent sequences of beds rather than a single layer [Moore, 1969]. In addition, it must be remembered that reflections result from changes in acoustic impedance. Although these changes commonly occur across lithologic boundaries, they may occur within lithologic units as well. Last, within the Canton Trough region, only the upper 20 m of sediments have actually been cored and rock samples were obtained at only one locality. Therefore, direct correlations of most reflecting horizons with lithologic units are not yet possible.

In this study, acoustic layers are distinguished from each other primarily on the basis of their reflectivity,

thickness, and relative position, and thus may be correlated with reflecting horizons and lithologic units described by other workers. Structural interpretations are based upon the continuity, thickness, attitude, and boundary contacts of acoustic layers. The fault symbols shown in Figure 5 do not necessarily indicate the proper attitude of fault planes, but are mainly for the purpose of locating inferred faulting.

C. Acoustic units

Although there are many reflectors traced in the profiles in Figure 5, they can generally be grouped into one of three acoustic units: a "transparent" layer, a stratified layer, and acoustic basement.

The transparent layer

The transparent layer exhibits extremely low reflectivity in the band-pass of 50-100 Hz and 150-300 Hz. At these frequencies, the layer is often characterized by a single faint reflection from the sediment-water interface (Figure 6 I) in contrast to the multiple reflections, indicative of stratification, occasionally observed within the transparent layer on 3.5 kHz echo sounder records.

Although often discontinuous and varying in thickness and in acoustic transparency, the layer occurs widely throughout the area. It is almost always found at depths

in excess of 5000 m where: (a) it may overlie "acoustic basement" as in Figure 6 I, where it shows its greatest average thickness (100 m - 200 m); (b) it may form a thin veneer over a highly stratified sequence, which is commonly separated from acoustic basement by yet another thicker transparent layer (Figure 6 III; the veneer is too thin to be seen at this scale but the lower transparent layer is obvious); or (c) it may appear as discontinuous pockets within stratified units (Figure 6 II, 6 III). Occasionally the layer is observed partially draped over topographic highs (Figure 5 and Figure 6 IV). The layer may be generally conformable to the unit below it, as in the basin on the southern side of Figure 6 I, but more often it has a smoothing effect on underlying topography, as shown in the northern basin in Figure 6 I. These patterns of occurrence indicate that the initial distribution of the transparent layer is strongly influenced by bottom currents.

The reflectivity of the transparent layer commonly varies laterally. For example, between points A and B in Figure 6 IV, the sediment-water interface gradually becomes more reflective downslope and a sequence of reflectors appears within the transparent layer, which becomes intermittently more reflective. Also the reflectivity may decrease where abrupt changes in basement topography cause the layer to arch (Figure 6 III and 6 IV at point C). In the narrow basin near the right side of Figure 6 III, a thick section

of stratified sediments is separated from the transparent layer by an almost vertical boundary. Wherever the transparent layer has been sampled within the Canton Trough region and the Central Pacific Basin, it has been found to consist predominately of radiolarian ooze. However, the aforementioned changes in reflectivity suggest that the layer is not compositionally monotonous. It is believed here that variations in reflectivity result from lateral changes in lithology involving varying degrees of contamination of siliceous ooze by other sediment types. The gradual changes in reflectivity (as in Figure 6 IV) represent rather gradual mixing downslope, whereas the distinct changes with near-vertical boundaries may represent a much higher degree of contamination, with the contaminate tending to be channeled along the deepest part of a basin. The contamination probably is due to turbidites repeatedly deposited along relatively fixed channels within the basins [Kroenke, 1970]. These turbidites form the stratified unit discussed in the following section.

The stratified unit

The stratified unit is recognizable in the area as a sequence of closely spaced, highly reflective, and nearly horizontal layers. This is easily seen in Figure 6 II, III, and IV. Where the unit is distinctly present, it is overlain

at the most by a very thin transparent layer. The unit is easily distinguished from acoustic basement when it is underlain by a transparent layer, as in Figure 6 III. Where the lower transparent layer is lacking or is too thin to recognize, the lower boundary of the stratified unit is more difficult to recognize.

For the most part the distribution of the stratified unit is restricted to two localities. These are (1) the eastern part of the northern basin labeled B in Figure 4, and (2) the broad, flat region south of the arch-like feature described previously (Figure 6 IV). Within the northern basin the unit is present from profile AA' through DD' in Figure 5, but its distribution there is variable. In profiles AA' and DD' (Figure 6 III is a photograph of this basin in profile DD') the unit is present across most of the basin, but in profile BB' - CC' (Figure 6 II) the stratified sequence occurs only within narrow channels near the middle of the basin. A relatively thick transparent layer separates these channels from each other. Although the northern basin is continuous beyond profile FF', the unit is not observed west of this profile. In profile FF' a thin stratified sequence may be present, overlain by a thicker transparent layer. The sequence here appears to be folded. There is some indication, at least in profile DD' and in Figure 6 III, that the stratified unit is actually two sequences of about equal thickness.

South of the arch-like feature the stratified unit appears as two sequences separated from each other and from acoustic basement by transparent layers (Figure 6 IV). These sequences combined are much thinner than the stratified unit observed within the northern basin. The continuity of the unit within this region is not definitely known, because most of the traverses did not extend that far south. However, stratified sequences were observed in profiles AA' and GG' (Figure 6 IV), and it may be assumed that they are present in the intervening profiles.

The stratified unit is believed to be composed of turbidites which flowed out from the higher elevations of the Line Islands Ridge. Similar conclusions have been reached by Kroenke [1970] for a region between the Canton Trough and the Line Islands. If this is the case, then the regions described here must be open to turbidite plumes from the northeast. Other basins in profiles AA' through MM', including the medial trough, lack these stratified sequences and are therefore closed to this type of deposition. The northern basin in profile FF' appears to be transitional between those open to the east and those closed to the west.

Acoustic basement

Whereas the terms "transparent" and "stratified," as used here, seem to have some correlation to lithology, the

term "acoustic basement" does not. It is used to denote the upper surface of the deepest continuous reflector, and, as such, has little overall lithologic meaning and should not be generally correlated with the term as used by Ewing et al. [1968]. Igneous rocks were dredged from the base of the southern ridge and presumably represent the composition of acoustic basement over the ridges. Away from the ridges, penetration within apparent basement increases as the presence of discontinuous deep reflectors becomes more pronounced (Figure 6 I and 6 IV). Although this is partly a result of the decrease in specular reflections associated with diminished topographic relief, the top of acoustic basement here is probably not igneous rock, but consolidated sediments. Horizon B, described by Ewing et al. [1968], may be the acoustic basement found here.

Ewing et al. [1968] and Ewing and Ewing [1970] show a reflection profile very near the Canton Trough in which they describe an opaque layer underlying a thicker transparent layer and overlying a thin transparent layer. The use of "transparent" by these workers is synonomous with its use here; but the term opaque has not been used. The southern part of Figure 6 IV is very similar to the section shown by Ewing and Ewing [1970, Figure 47], and it is likely that the stratified sequences here are correlative with these workers' opaque layer.

D. Structure

The bathymetric lineations shown in Figure 4 can be divided into three structural provinces. These have been termed the northern, central, and southern provinces [Rosendahl and Halunen, 1971].

The northern province includes all topographic features occurring north of the major ridges and medial trough and lying between about 167°W and 169°W. The region has an unmistakable block-faulted character with topographic highs and lows appearing as horsts and grabens. The northern basin seen in profiles AA' through GG' and discussed previously is believed to be a graben. This structure, 30 to 35 km wide, is composed of a main graben separated from a much narrower one by a small ridge. In profile AA', these structures are at the same elevation, whereas in more westerly profiles the narrow graben occurs at a deeper level. The northern boundary of the main graben has also been step-faulted in profiles BB' through GG'; it is entirely shown only in profiles BB' and CC' and in Figure 6 II and 6 III. Faulting may also have occurred within the main graben as seen by the offset stratified sediments along the center line of Figure 6 III (profile DD'). To the north, this graben is flanked by a prominent horst (profile AA') that narrows to the west. Continuing farther north the structure is like that shown in Figure 6 I. Downfaulted blocks here are 10 to 12 km wide and may be tilted. Although data

are largely lacking, the structural continuity of the region shown in Figure 6 I does not compare with structures farther south.

In profile LL', the southern part of the northern province is apparent, but this profile as well as those west of it failed to extend far enough to the north to delineate the remainder of the structure. In profile MM' and traverse NN', the extreme relief of the province has largely disappeared.

The central province includes the major ridges and axial trough.and is therefore the most topographically prominent of the three provinces. As previously pointed out, the morphological development of the southern ridge and axial deep attains a maximum along profile GG' and traverse HH' and apparently this is inverse to the development of the northern ridge. Along profile LL', the southern ridge has apparently been downfaulted about 1 km relative to its position with respect to other blocks. The axial trough here also appears to be fault-widened. West of profile LL' the central province rapidly loses its extreme topographic expression and in traverse LM' and profile MM' the trough is the only remaining structure of any significance. Here it is poorly developed and is as wide as it is deep. In the most westerly traverse (traverse NN' in Figure 2 or Section N, Figure 18) an offset occurs along the strike of the axial trough. This structure, shown as a scarp in Figure 4, may

be continuous with the central province or it may be associated with the seamounts in this region.

The southern province includes all structures south of the central province in profiles AA' through LL'. The most prominent structure here is the arch-like feature bordered by a small graben to the north and a wide, flat, undeformed basin to the south. The northern boundary of the arch is probably step-faulted, as is best seen in profiles DD' and EE'. Faulting along the southern boundary is suggested only in profile GG' and, if generally present, occurs at lower angles than faulting along the northern edge. The arch-like shape is not observed in traverses II', JJ', and KK' or in profile LL', but this may be a result of changing fault patterns. For instance, Section I (topographically equivalent to traverse II, Figure 2) in Figure 15 shows a gentle slope from the southern ridge to the basin and is similar to the reflection record along traverse JJ'. Apparently the small graben has not developed here. However, in traverse KK' and profile LL', the extreme opposite may be true; the small graben here may be vertically displaced as much as 1 km. In any case, the structure south of the arch, at least in profiles AA' and GG', is subdued with respect to the other regions, and apparently indicates much less intense crustal stress there.

The southern ends of traverse LM' and profile MM' are characterized by seamounts. The region between the axial

trough and the seamounts, shown along profile MM', is of low relief but sediments are folded and acoustic basement faulted in at least one locality.

From the descriptions of these provinces it is apparent that faulting plays an important role in their morphology. This is especially evident in the northern province where the physiography may be almost entirely a consequence of block faulting. The major ridges within the central province are thought to be largely of igneous origin. Possibly fracturing was extreme there, allowing intrusion and volcanism to occur along the boundaries of a downfaulted block. If it is assumed that the axial deep is a remnant of this block, downfaulting may have exceeded 2.5 kilometers. In the southern province, faulting is prevalent on the northern side of the arch and less so on the southern. The arch itself may be an upfaulted block, possibly tilted towards the south. Faulting generally appears to be tensional and the fault patterns associated with the central province may be en échelon. Although this can be explained by several mechanisms, the simplest is probably a shear couple. Strike-slip motion within this region, if present, is not indicated by conventional means, such as offset bathymetric and magnetic lineations or the presence of regional changes in depth across the feature; however, this is not necessarily conclusive evidence that transcurrent motion has not occurred here. Future detailed mapping with

traverses parallel to the Canton Trough trend would be needed to delineate strike-slip motion.

Secondary structural patterns are not clearly displayed in this region because most traverses cross the primary lineations nearly perpendicularly. There are indications, however, that some minor bathymetric lineations trend sub-parallel to the Phoenix Islands. For instance, contours in Figure 3 at 169°W and 1° 25'S suggest the presence of a structure trending obliquely across the main lineations.

GRAVITY

A. General

During the R/V MAHI survey of the Canton Trough region, gravity data were obtained at 292 stations along approximately 1400 km of ship traverses (Figure 7). Gravity measurements were made using a La Coste and Romberg gimbal-mounted sea gravimeter S-3. This instrument required values to be averaged over 10-minute intervals, although in this study data points generally correspond to 15-minute intervals. On several sections of the ship's track, sea conditions did not permit valid measurements.

Track-crossing checks on accuracy are not available and therefore the accuracy of values between traverses is unknown. The accuracy within any continuous traverse is estimated at ± 5 mgal (J. C. Rose, personal communication).

As part of a continuing program of gravity compilation and reduction at the Hawaii Institute of Geophysics, all principal facts related to gravity measurements are digitized for computer printout format. In addition to including date, time, coordinates, and corrected water depth, the free-air and simple Bouguer anomalies are routinely computed. The Bouguer anomalies are computed for crustal densities of 2.60 and 2.87 gm/cm^3.

In this study gravity anomalies are ultimately correlated with sub-bottom geologic structure. Bouguer anomalies, as

such, were found to be dependent upon topography and it was therefore necessary to compute residual gravity anomalies for this purpose. From residual and free-air anomalies, generalized crustal models were constructed.

B. Computation of residual anomalies

Theory

Several types of gravity anomalies are applicable for the study of geologic structure. The relevant types for this study are those in which surficial effects (topography) are at least considered, and preferably, removed. The free-air anomaly is a result of combined topographic and geologic effects. In oceanic regions of low relief and constant depth and sediment thickness, the free-air anomaly is a direct indicator of sub-bottom geologic variations. But in regions of relatively high relief and complicated structure, such as the Canton Trough, free-air anomalies are inadequate as indicators of sub-bottom structure. The simple Bouguer correction at sea substitutes crustal rock of appropriate density for the volume occupied by the water layer. In effect, the Bouguer calculations correct the free-air anomalies for the deficiency of mass caused by the presence of a water layer. However, simple Bouguer anomalies over large topographic features, such as seamounts, commonly show an inverse relationship to relief when normal crustal densities

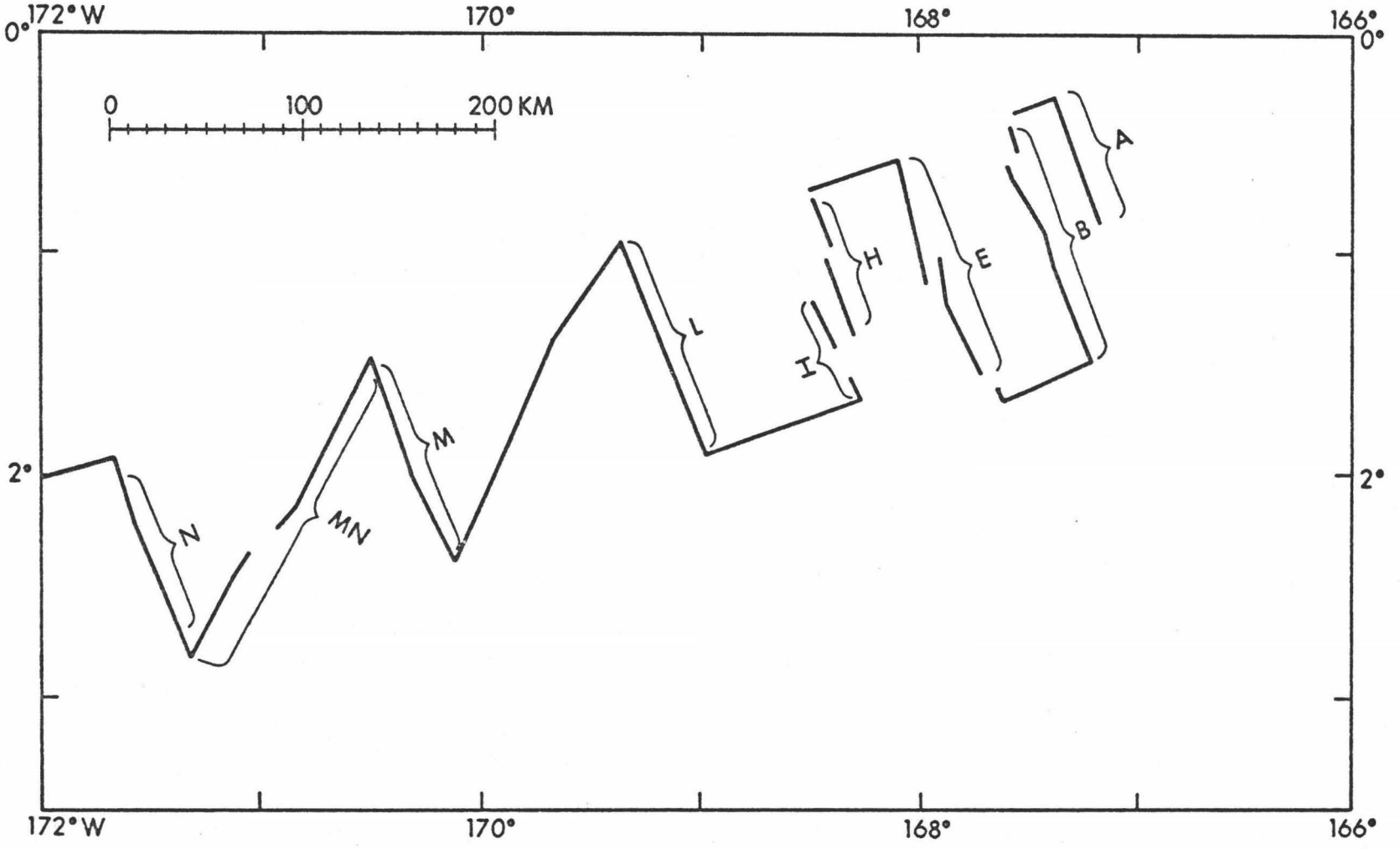

Fig. 7. R/V MAHI traverses along which gravity data were collected. Lettered segments indicate location of gravimetric sections shown in Figures 8 through 18.

are used in the correction [Harrison and Brisbin, 1959]. In such areas there is still a topographic component to the anomaly. In addition, Bouguer corrections do not normally take into account local changes in density due to sediment layers. Simple Bouguer anomalies within the Canton Trough region were found to be extremely dependent on topography and thus were not significantly more useful in structural interpretation than the free-air anomalies (Figure 8).

If the distribution of anomalous mass is to be used to aid the interpretation of sub-bottom geology, the mass of the known features or layers must first be computed. The resultant value can then be subtracted from the free-air anomalies to eliminate the effect of the known features. The remaining anomaly is termed the residual anomaly.

Previous work

The computational procedure used in this study has as its underlying assumption that geologic structure can often be considered two-dimensional. The application of two-dimensionality to gravity analyses [Nettleton, 1940] has given rise to various methods of computation of the gravitational attraction of two-dimensional bodies. These include graphical methods, such as graticules [Hubbert, 1948] and mathematical calculations using simplified geometric shapes [Vening-Meinesz et al., 1934; Shurbet et al., 1956; Talwani et al., 1959a].

The method devised by Talwani et al. [1959a] forms the basis of the procedure used here. This method assumes that the gravitational effect of any two-dimensional body can be approximated by breaking it up into a many-sided polygon. The corners of this polygon are defined in a Cartesian coordinate system and the attraction of the polygon computed using a line integral along some datum level. Digital computer methods permit such computations to be performed extremely rapidly. Using this two-dimensional method, the gravitational effect of any layer can be computed. Subtracting the effect of that layer from the observed free-air anomaly profile theoretically removes the gravitational effect of the layer. In this fashion, the attraction profiles of the water layer, sediment layers, and crustal layers can be theoretically computed and subtracted from the free-air anomaly profiles to obtain a residual anomaly [Talwani et al., 1959b].

Qualitative procedure

Although the method employed here follows that described by Talwani et al. [1959a, 1959b], the residual anomalies computed in this study are not synonomous with those computed by these workers. The residual anomalies computed and described by them [1959b] are certainly adequate as indicators of sub-bottom structure, but their procedure cannot be explicitly applied to the Canton Trough region.

These workers constructed crustal sections using both seismic refraction and gravity data. There is a complete lack of seismic refraction data within this study area and consequently the delineation of sub-bottom layer boundaries is practically impossible at this time.

Without seismic control, topography cannot be considered as a continuous layer, the effect of which can be removed by a two-dimensional computation. However, since topography usually contributes to observed gravity, it can be reasoned that the occurrence of topographic features above some modal water depth would contribute a positive component to the free-air anomaly profile. Similarly, sediments found above this modal depth would also contribute a positive component to the anomaly profile. If there is a lack of topography, such as in a trough, or the presence of sediments below this modal depth, then a negative component would be contributed to the free-air profile. In this fashion a section can be reduced to a two-layer model consisting of water (from sea level to the modal depth) and crust (deeper than the modal depth), with no relief between the layers.

For the Canton Trough region, a modal water depth of 5.4 km has been chosen. Negative corrections were added to the free-air anomaly profile for topography and sediments occurring above this level, and positive corrections for water or sediments below. These corrections were computed on the University of Hawaii computer using a program version

by Gemperle of Oregon State University. The mechanics involves assigning negative and positive densities to negative and positive corrections, respectively. Thus positive components have negative corrections because negative densities are assigned to them. The profile obtained from plotting the correction factors is termed the correction anomaly profile. Adding this profile to the free-air profile yields a residual anomaly profile. Residual anomalies obtained by this method can be considered "complete" free-air anomalies, and can be regarded as equivalent to land-based complete Bouguer anomalies.

Density determinations for correction anomaly calculations were obtained in several ways. It is generally believed that a normal crustal density of about 2.87 gm/cm^3 is too high for most marine bottom topography. In this study, correction anomalies have been computed for constant topographic densities of both 2.50 gm/cm^3 and 2.30 gm/cm^3. Section A of Figure 8 shows there is not a significant difference in the residual profiles computed for these densities. Similar conclusions have been reached for all other sections in Figures 9 through 18 and thus only profiles using the 2.50 gm/cm^3 density are shown. Sediments within most of the Canton Trough region are composed mainly of radiolarian oozes and turbidites. Compressional velocity measurements on these types of sediments indicate typical velocities of 1.50 to 1.60 km/sec (Initial Reports DSDP VII).

Using a Talwani, Nafe-Drake velocity-density curve [Talwani et al., 1959b], this range is equivalent to densities of 1.60 to 1.70 gm/cm^3. The 1.70 gm/cm^3 value has been used here. In sections MN and N, Figures 17 and 18, the sediments on the southern part of the sections are suspected to be shallower water calcareous sediments, and a density of 2.1 gm/cm^3 has been assigned to them. A density of 1.03 gm/cm^3 has been used for sea water.

C. Construction of crustal models

Theory

Talwani et al. [1959a, 1959b] have used the residual anomalies computed by them to construct crustal models. They employed the line-integral method to compute the gravimetric attraction of a section from sea level to the Mohorovicic discontinuity. By adjusting only the depth of the Moho, their attraction profile can be made to fit their residual anomalies. They also computed the total attraction of a section from sea level to some compensation depth (32 km). Again by adjusting only the Moho, the mass attraction can be made to fit the free-air anomalies after subtracting an attraction constant. Although the two methods are equivalent, the second has been used here, due to the inherent difference between the residual anomalies computed by those workers and by the present writer.

Qualitative procedure

To compute the attraction profile of a crustal section, a model with the Moho at an arbitrary depth is constructed from sea level to a depth of 32 km. The attraction at sea level is computed along the section at 2-km intervals. A constant is then subtracted from all the 2-km values, and the remaining values are plotted with respect to the free-air profile. By adjusting only the Moho boundary, the attraction profile can be made to fit the free-air profile.

The constant used here was determined by computing the total attraction, from sea level to 32 km depth, of a known seismic refraction section. Ideally the known section should be a standard crustal model within the pertinent region and over which the free-air anomaly is a known quantity. Although not in the immediate study area, a seismic refraction section has been determined by workers from the Hawaii Institute of Geophysics [Sutton et al., 1970, Section Number 7, Figure 10] which may be construed as representative of the general region. This section is located at 02°23'N, 162°50'W, or about 140 km north and 560 km east of the major ridge seen in profiles AA', Figure 4 and A, Figure 8. Using the Talwani, Nafe-Drake curve [Talwani et al., 1959b], appropriate densities have been assigned to the layer velocities and a total attraction of 3929 mgals was computed. The observed free-air anomalies over this section average near-zero. Therefore no adjustment in datum is required and this value

can be used directly as the constant subtracted from the interval determinations.

D. Interpretation of gravity anomalies and crustal models

Errors

Theoretically, the residual anomalies computed in this study should have all topographic and sedimentary effects removed from them and should reflect only variations in sub-bottom structure. As a consequence of (1) mechanical problems, (2) edge effects, (3) failure of the two-dimensionality assumption and (4) lateral variations in the density of topographic features, this is not always so.

Mechanical problems include actual errors in the measurement of gravity and errors introduced in the free-air anomalies by the use of invalid reduction parameters. Edge effects are topographic errors introduced near the ends of sections. They are generally reduced as much as possible in the calculations by effectively continuing the section to infinity. However, topography away from the immediate ends of sections is often totally unknown and cannot be considered in correction calculations. Although an assumption of two-dimensionality is certainly valid on a large scale for traverses perpendicular to the strike of the Canton Trough, the assumption partially or completely breaks down for traverses which are oblique or parallel to the trough and

even for local segments of several of the transverse sections. Actual lateral variations in topographic density are not considered in initial calculations of the correction anomaly, since these are computed for constant topographic densities. Almost certainly this introduces small local errors in some residual anomaly profiles.

Determination of geologically controlled residual anomalies

The criteria for distinguishing between possible geologic and non-geologic residual anomalies are primarily dependant upon anomaly wavelength and amplitude. Since these factors are largely controlled by density and distance from the source, theoretical anomaly profiles provide at least an estimate of the expected anomaly generated by some body at a given density and depth. Although these profiles can be computed for an infinite number of bodies by varying their size, shape, and density, limits are imposed here by water depth and reasonable density contrasts. In this fashion, the minimum wavelength and maximum amplitude can be computed for reasonable sub-bottom variations. These extremes can also be estimated from the correction anomaly profiles. The maximum density contrast for geologic structure is presumed to be at the Moho between mantle rock and crustal rock ($3.44 - 2.50 = 0.9$ gm/cm^3), a contrast that is less than that at the sea floor between crust and water ($2.50 - 1.03 = 1.47$ gm/cm^3). It follows that bottom topography, being

nearer to sea level and having a larger density contrast, should normally generate larger amplitude, shorter wavelength anomalies than would local sub-bottom geologic structure. Although variable, residual anomalies having wavelengths shorter than 20 km usually cannot be generated by reasonable variations in either shallow structures or in the depth to Moho.

Residual anomalies of possible geologic origin are next examined with respect to the aforementioned errors. If these measures fail to eliminate the anomaly it is presumably generated by sub-bottom sources. This process of elimination has been carried out for all residual anomaly profiles shown in Figures 8 through 18.

Geologic sources of residual anomalies

In the absence of seismic control, geologically significant residual anomalies may be attributed to any number of sources. These include isolated sub-bottom bodies such as intrusions, variations in density or thickness of sub-bottom layers, and variations in the total thickness of the crust. Bullard and Cooper [1948] have used the wavelength and amplitude of gravity anomalies to devise mathematical methods by which the maximum depth of an anomaly's source can be determined. Although these "maximum depth rules" could be applied to the analyses of residual anomalies, they would not eliminate any of the possible

sources listed above, because residual anomalies of geological significance are usually long-wavelength and distorted, with the exact density contrasts of the source unknown.

As an initial approach toward interpretation, the residual anomalies are arbitrarily assumed to originate from variations in crustal thicknesses. Using the residual anomaly profiles as guidelines for the general location and extent of these variations, crustal models are constructed to fit the free-air profiles. In this sense the residual profiles exercise some control by limiting the number of Moho configurations that could normally be made to fit the free-air profile. If the crustal models appear reasonable, then the major geologic variations are presumed to result from changes in crustal thicknesses. However, if the models demand extreme fluctuations in the depth to the Moho in order to match the free-air profiles, then the sources of anomalous mass are probably within the oceanic crust. In the construction of the initial models it is assumed that the crust is a single homogeneous layer of 2.88 gm/cm^3 density and varying only in thickness.

E. Results

Gravimetric sections

The interpretation of geologic structure for gravity anomalies throughout the Canton Trough region is based on gravimetric sections A through N (Figure 7). The topographic profiles shown in these sections are digitized equivalents

of seismic reflection profile tracings, most of which are shown in Figure 4. The location of these sections is shown in Figure 7.

Section A

This section, shown in Figure 8, is a plot of free-air, residual, Bouguer, and correction anomalies. The free-air profile directly reflects topography with a +18 mgal maximum over the ridge and a -32 mgal minimum near the northern edge of the basin. The correction anomaly profile is approximately the inverse of the free-air profile, and for all practical purposes the major relief of the latter can be largely attributed to topography. The residual anomaly profile is negative across the total section, reaching a -38 mgal low over the central province. The profile can be smoothed by allowing the topographic density to vary slightly. For instance, by assigning a density of 2.30 gm/cm^3 to the central province while retaining a density of 2.50 gm/cm^3 for surrounding material, the residual profile becomes nearly constant at -30 to -35 mgals. If topographic density is kept constant, there appears to be a slight mass deficiency beneath the central province. In either case the residual profile implies a regional mass deficiency which may indicate a depressed mantle across the whole section. Figure 9 shows a model that fits the free-air profile adequately.

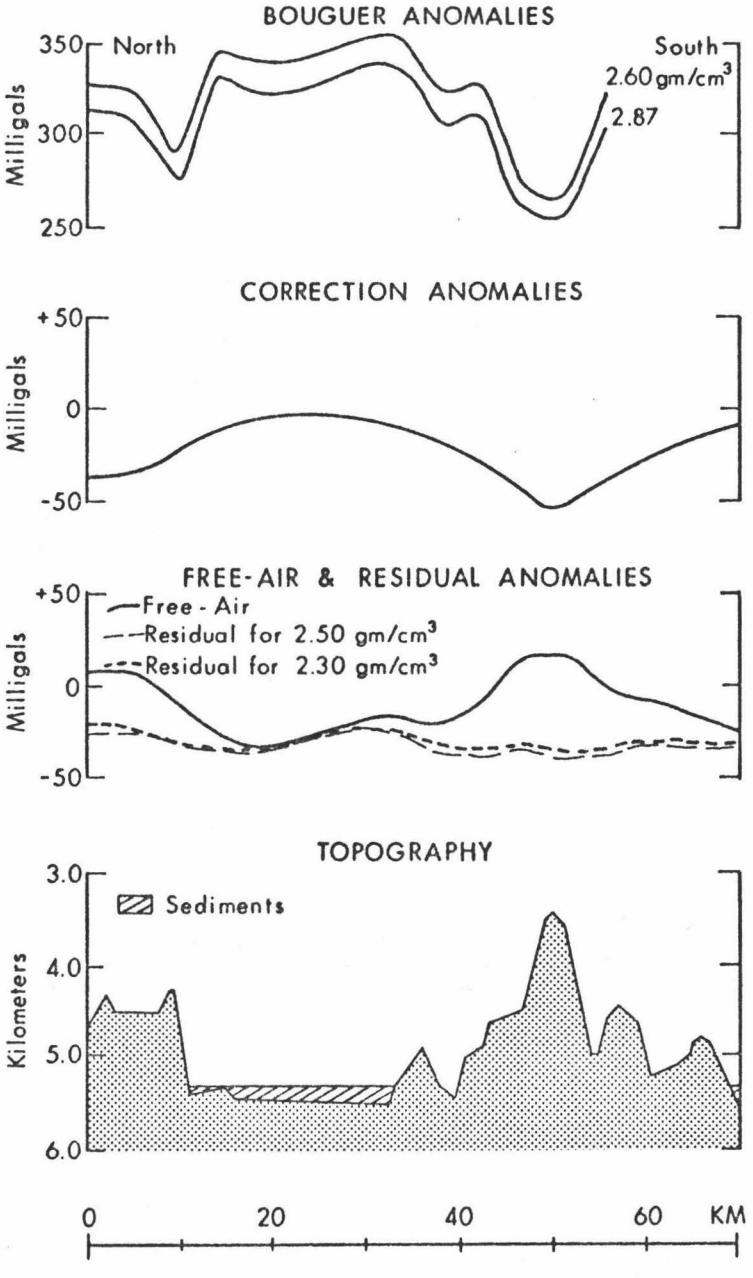

Fig. 8. Gravimetric section A.

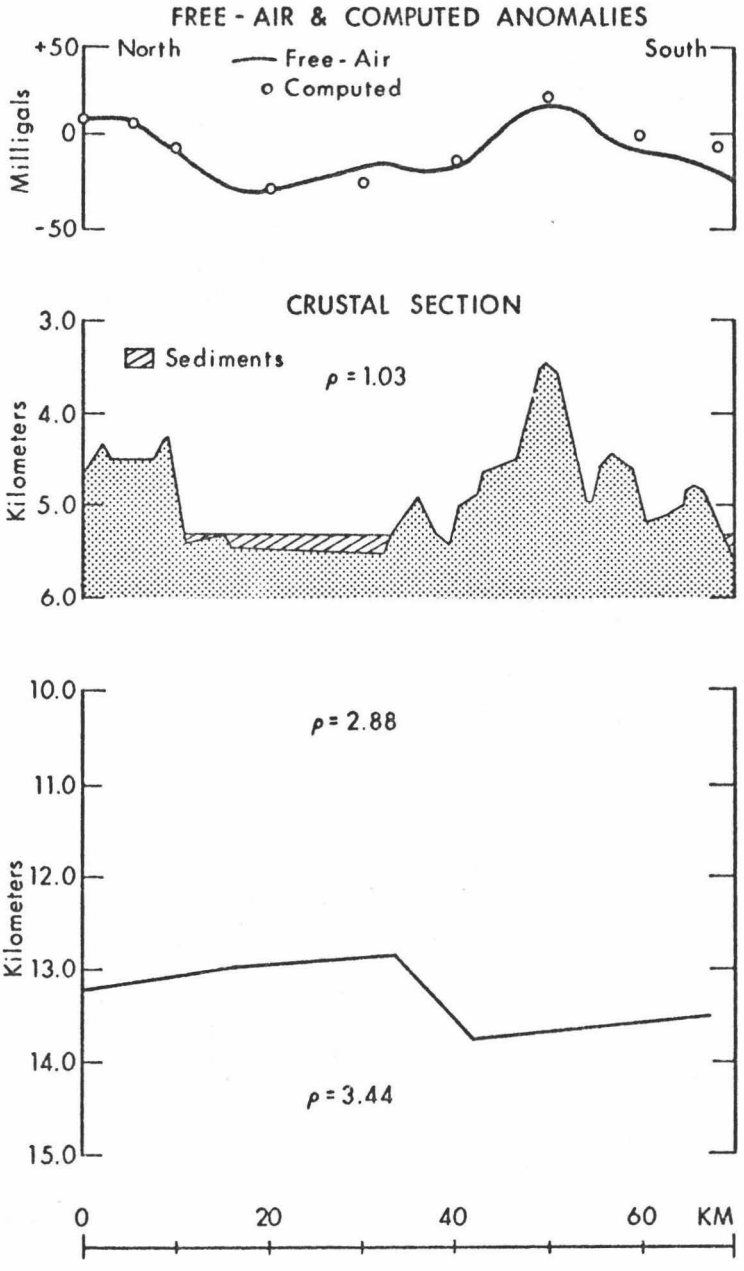

Fig. 9. Crustal model for section A.

Section B

Figure 10 shows a plot of free-air, residual, and correction anomalies along section B. The topographic profile here is a composite of seismic reflection profile tracings BB' - CC' shown in Figure 4. The correlation between topography and free-air anomalies is quite poor and completely breaks down over the major ridges. The correction anomaly profile also shows a negligible effect over these features. Apparently the geometry here is such that the deficiency of mass of the trough is roughly compensated by the added mass of the ridges. In addition, a bias is introduced here because the sampling interval falls over the flanks of the ridges, further reducing the observed effect. Even with this explanation, the free-air profile is largely problematical. Most of the short wavelength anomalies show up in the residual profile. These cannot be generated by reasonable sub-bottom structure and need not be considered further.

The geologic significance of the residual profile lies in its trend. The region north of the southern ridge which displays a negative residual anomaly is the morphological equivalent of section A. The negative anomaly can be interpreted as a region of thicker crust. South of this ridge the positive anomaly corresponds to a region of excess mass. If attributed to variations in mantle depth, this excess indicates an elevated Moho. A possible interpretation is shown in Figure 11. In order to fit the large positive

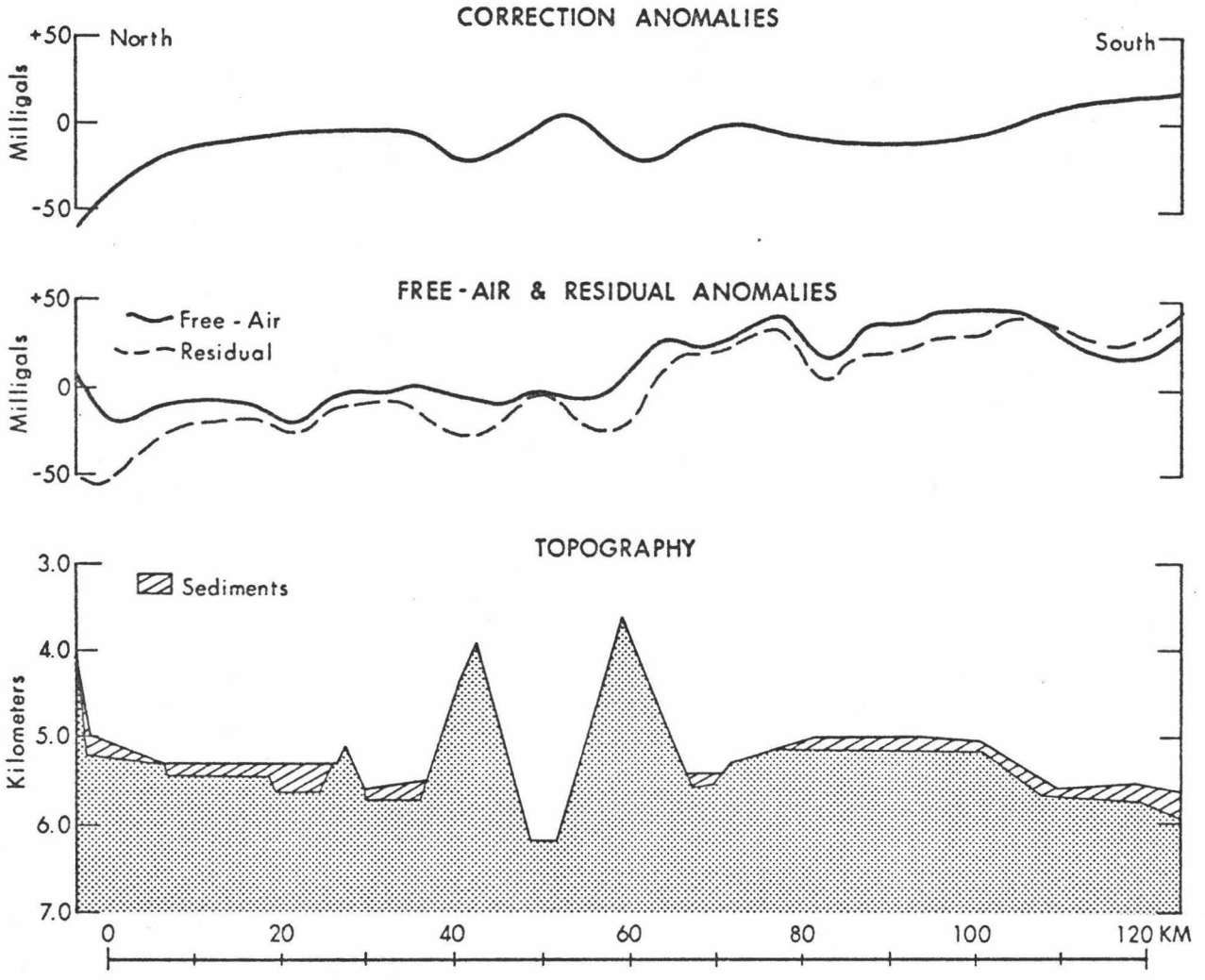

Fig. 10. Gravimetric section B.

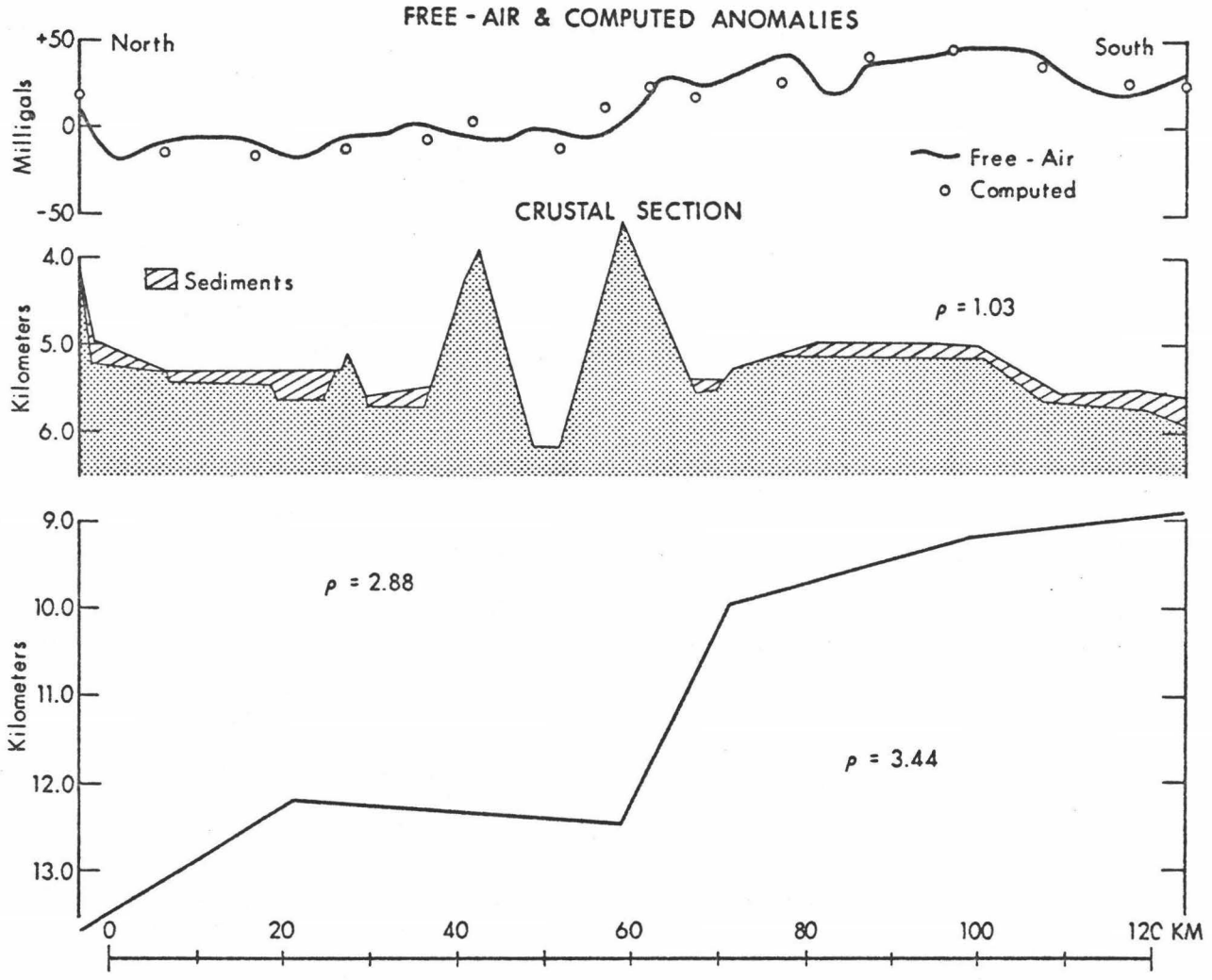

Fig. 11. Crustal model for section B.

free-air anomalies, thin crust is needed on the south side of this model. Alternatively, the arch-like feature in this section and in reflection profiles AA' through GG' (Figure 4) may represent the topographic expression of a denser pluton within the crust. Using a crustal density comparable to that of the gabbros dredged from the Canton Trough (2.88 gm/cm^3) and a funnel-shape extending to 11.5 km depth, the positive residual anomaly can largely be accommodated. Unfortunately, gravity data for additional modeling are lacking over the corresponding feature in section AA' and along the complete length of the adjacent western traverse.

Sections E, H, and I

Although separated from one another by as much as 60 km, these sections are quite similar. Figures 12 and 13 show plots of free-air and residual anomalies. A possible crustal model is also shown for section E, which is probably applicable to sections H and I.

There is a strong correlation between the major topographic features and free-air anomalies. Over the southern ridge, free-air anomalies are as large as +50 mgals in section H, whereas the medial trough is characterized by anomalies as negative as -115 mgals in section I. Other features have only minor local expression. There are three small regions where data are missing. Two of these are located over equivalent topographic features along sections

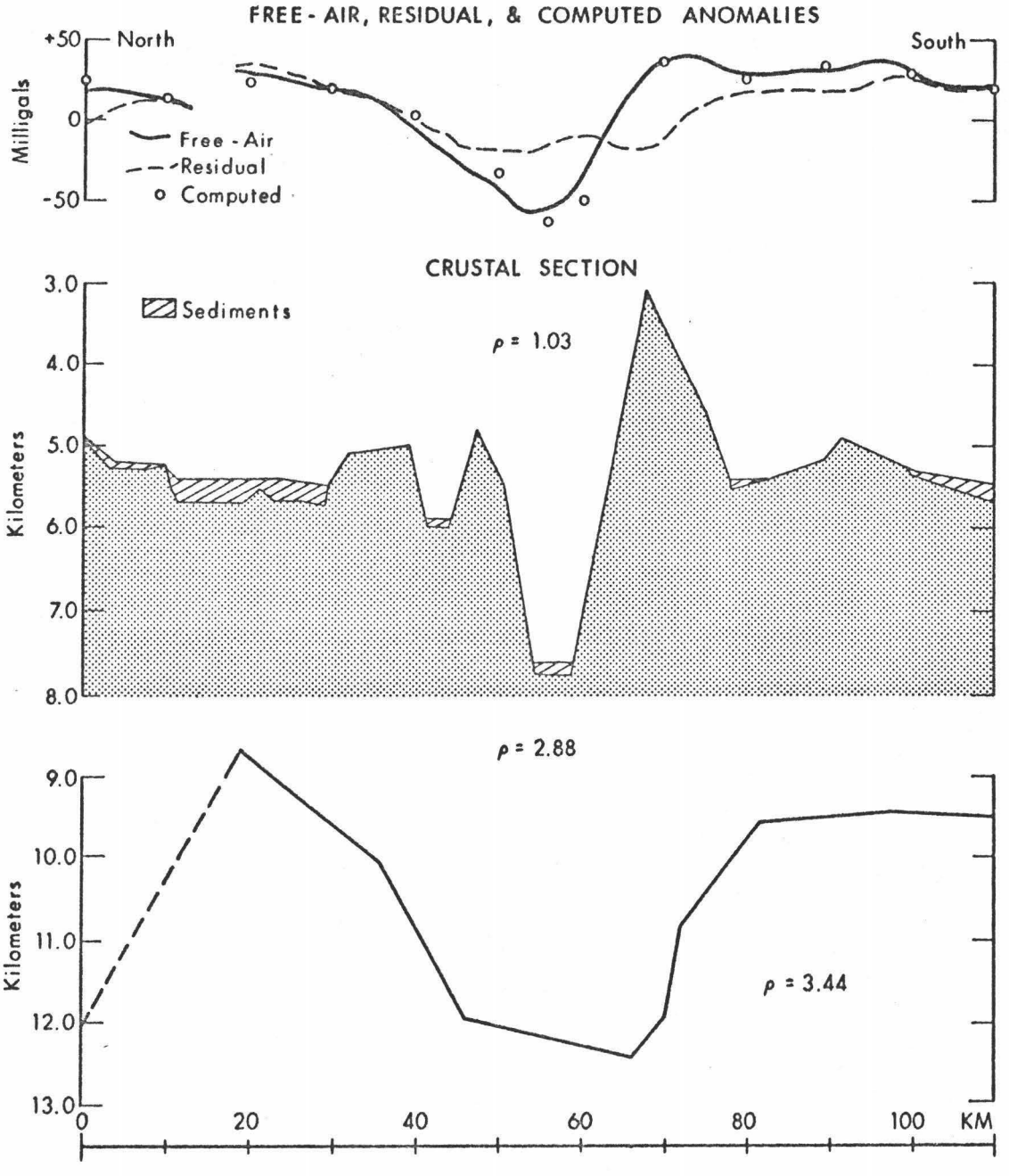

Fig. 12. Gravimetric section E with crustal model.

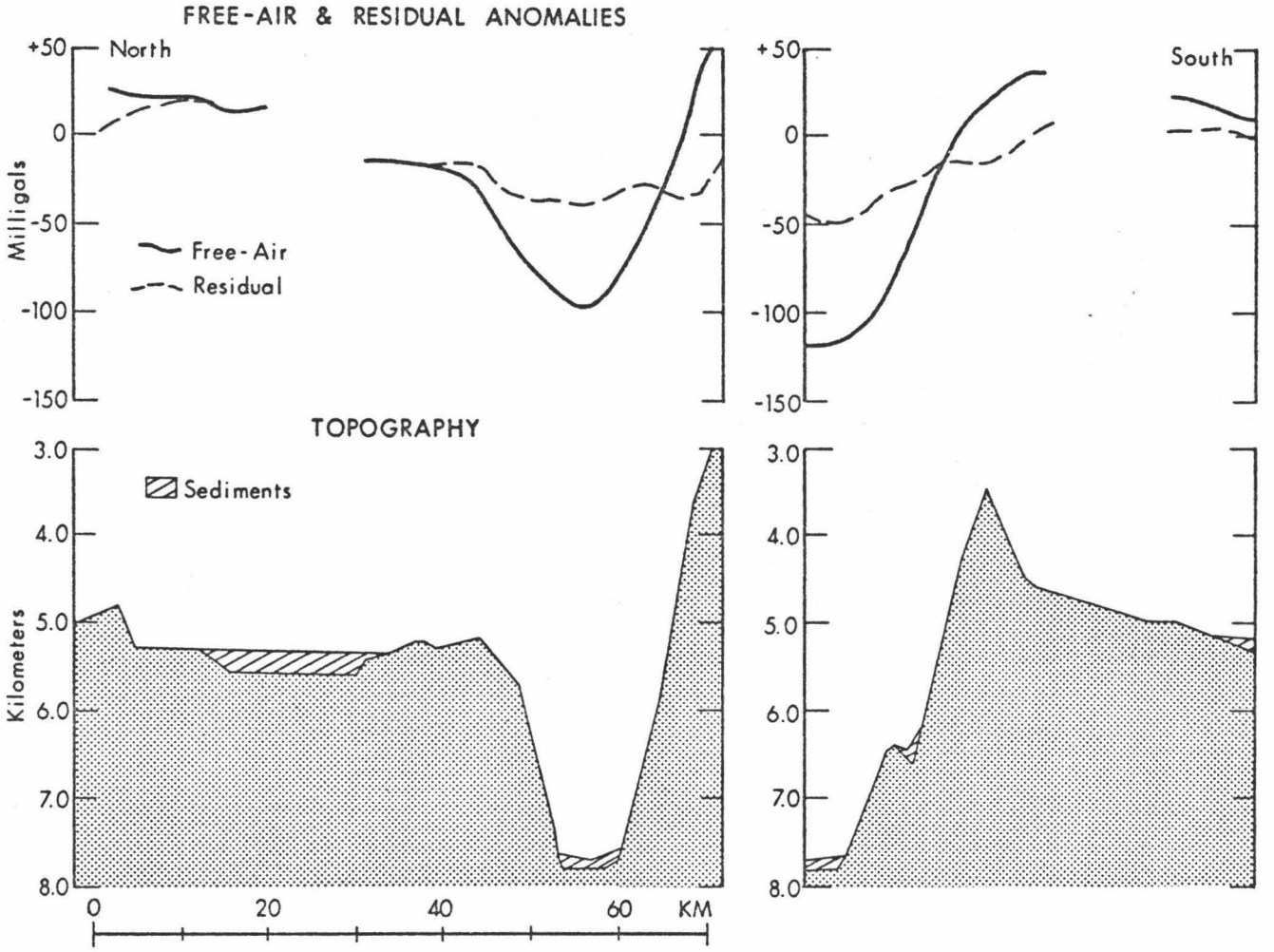

Fig. 13. Gravimetric sections H (left) and I (right).

E and H and both are problematical. These two areas indicate abrupt anomaly offsets that are opposite to each other. Neither has any direct topographic relationship. The offset in section E cannot be generated by any reasonable geologic phenomenon and it is presumed to be a mechanical error. The short section of profile north of this gap is suspect for this reason. The data gap in section H was caused by a breakdown in ship's power and the gravity anomaly offset, if real, is probably not as steep as indicated here.

The residual anomaly profiles in these sections show a broad negative anomaly flanked by positive anomalies. The negative anomaly is everywhere wider than 30 km and characterizes the central volcanic province. It appears strongly bimodal in sections E and H and less so in section I, where it reaches a minimum of -49 mgals. The bimodal nature is believed to be artificially generated and can be partially eliminated by allowing the topographic density to vary laterally. Again, assigning a density of 2.30 gm/cm^3 to the southern ridge (which is thought to be volcanic) and retaining the 2.50 gm/cm^3 density for surrounding material, the anomaly is reduced to something similar in form to that in section I. The remaining negative residual anomaly cannot be eliminated by any non-geologic considerations and presumably represents a mass deficiency. Similarly, the flanking positive anomalies, although problematic in the areas previously mentioned, cannot be largely eliminated and probably represent relative mass excesses.

The residual profile can be simply explained by postulating a compensating root beneath the central province and adjusting the Moho boundary to fit the free-air profile. This model is shown in Figure 12. Similar models with deeper roots could be constructed for sections H and I.

A depressed mantle beneath the central province and elevated mantle south of it substantiates the model shown for section B in Figure 11. However, the depressed mantle shown on the north side of sections A and B is incongruent to the elevated mantle in this section. Since the structure north of the trough is almost certainly continuous, the Moho change implied here is difficult to comprehend. The alternative explanation requires substantial lateral density variations within the crust. Such a situation is equally improbable for this area. This problem cannot be resolved with the data presently available.

Section L

This section, shown in Figure 14, is a plot of free-air, residual, and correction anomalies. The free-air profile exhibits an extremely sharp, -65 mgal anomaly centered over the northern edge of the trough. A gentler positive anomaly characterizes the southern ridge. There is also a short-wavelength, high-amplitude positive (+45 mgals) anomaly near the southern edge of the trough. This anomaly has no corresponding topographic feature.

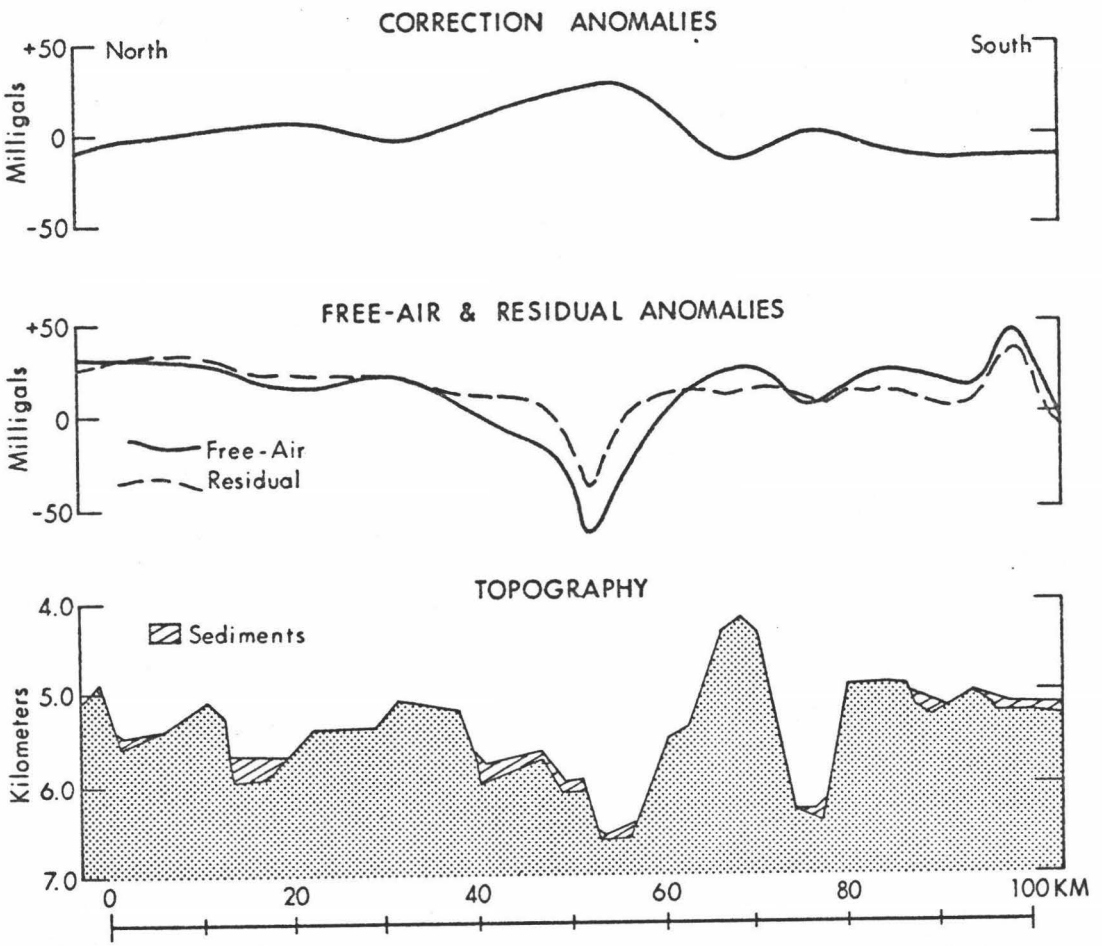

Fig. 14. Gravimetric section L.

The correction anomaly profile shows the inverse theoretical topographic effect across this section. It is apparent that the -65 mgal free-air minimum is only partly generated by topography, as the residual anomaly here is still a -40 mgal low. The +45 mgal free-air maximum shows up as a +35 mgal residual anomaly. These residual anomaly extremes have very short wavelengths with respect to their amplitudes, and attempts to generate these anomalies using reasonable structures and densities proved unsuccessful. The wavelength of the -40 mgal residual minimum can be somewhat lengthened by assigning a density of 2.30 gm/cm^3 to the major ridge, but the anomaly is still geologically unrealistic. Apparently these residual anomaly extremes are largely a consequence of non-geologic factors. Neglecting these anomalies, the residual profile shows a regional gradient from +35 mgals near the northern end to about zero at the southern end. This change is probably geologic in nature and is rather easily explained by a southward-thickening of the crust. Figure 15 shows the fit of such a model to the free-air profile.

The structure delineated by seismic reflection profiling is substantially different here than that in more easterly sections (section L has less topographic relief but is apparently more faulted). If the crustal models have any validity, this change may involve Moho configurations as well.

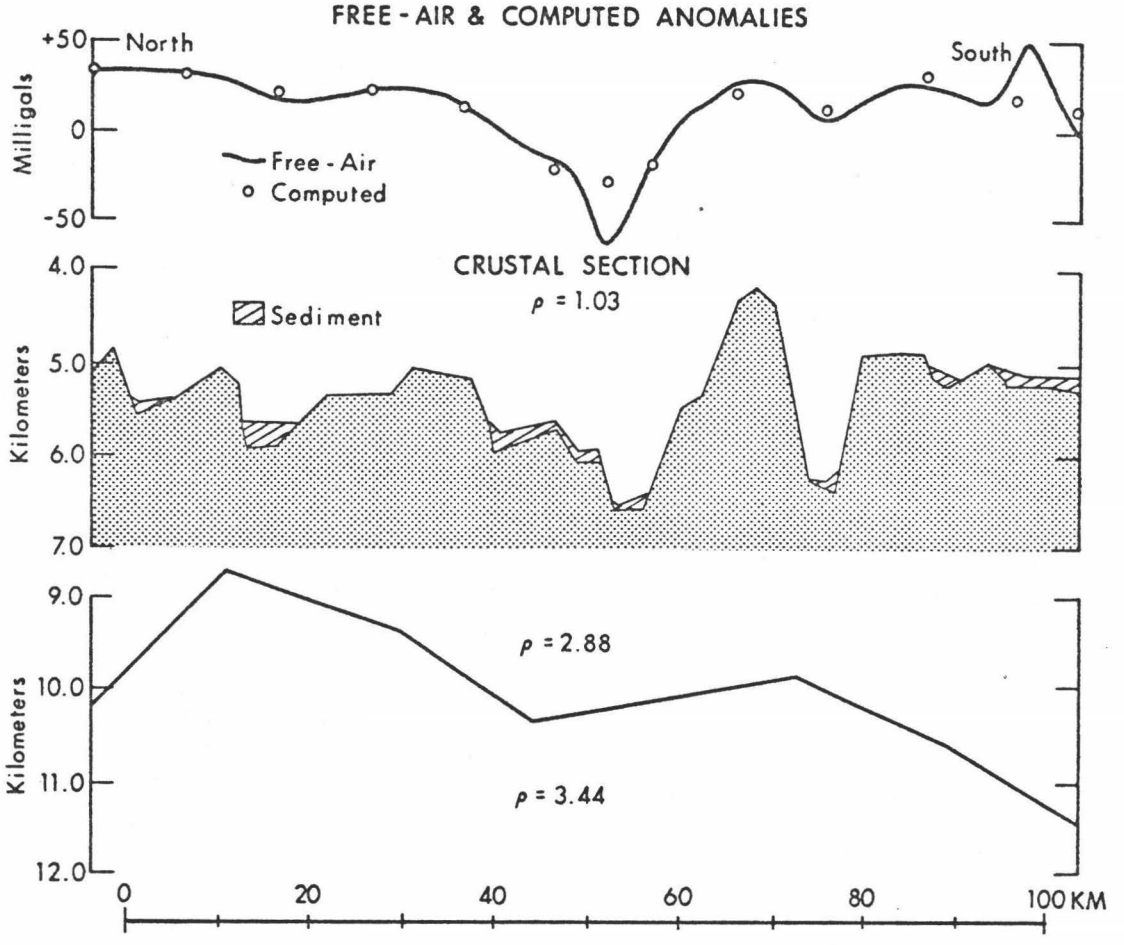

Fig. 15. Crustal model for section L.

Section LM

This section has not been shown, although it connects transverse sections L and M. The topographic relief along this section is large enough to generate significant anomalies. For this reason and because it crosses the bathymetric lineations at an oblique angle, section LM cannot be considered two-dimensional. It is sufficient to state that the residual profile across LM is a series of non-geologically controlled, short-wavelength anomalies superimposed upon a regional gradient similar to that discussed for section L.

Section M

This section, shown in Figure 16, is a plot of free-air and residual anomalies. A crustal model is also shown. With the exception of the seamount, the topography here is rather subdued and has only a minimal effect on the observed gravity. The free-air maximum is +35 mgals and occurs over the seamount on the south side of the section. There is no distinct free-air minimum.

The residual profile is also smooth. A broad, negative residual anomaly is centered over what is presumably the medial trough. A -25 mgal residual anomaly is associated with the seamount. Positive anomalies occur between these negatives and near the northern end of the section.

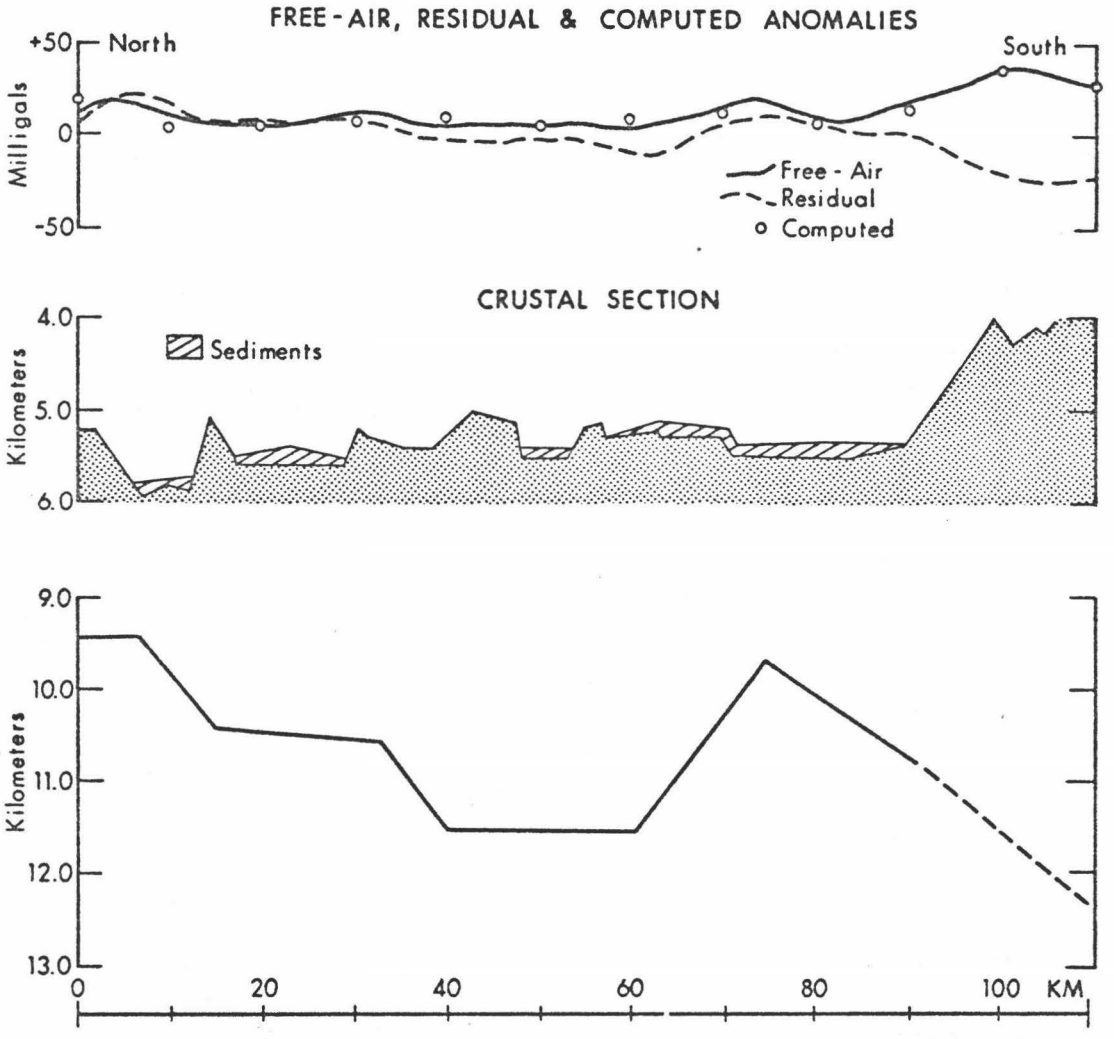

Fig. 16. Gravimetric section M with crustal model.

The positive and negative residual anomalies located on the northern and southern ends, respectively, are almost certainly generated by non-geologic factors. For example, the negative associated with the seamount shows a local breakdown of the assumption of two-dimensionality. The free-air profile over this feature is about half as large as the theoretical anomaly, a relationship that would be expected for a two-dimensional assumption for a three-dimensional feature. The residual anomaly here should probably be near zero. The positive anomaly over the northernmost basin has a wavelength too short to be generated by any sub-bottom variations.

The residual profile between these non-geologic anomalies appears to reflect real sub-bottom variations, since topographic relief here is too low to introduce significant two-dimensionality problems or variable errors in topographic density. Assuming that the residual anomaly over the seamount should be near zero, the residual profile shows a small, broad negative anomaly flanked by positive anomalies. This pattern suggests a central region characterized by lower sub-bottom densities or a thicker crust. Figure 16 shows a possible model that is not greatly different from that shown for section L (Figure 14).

Section MN

This traverse, like traverse LM, crosses the strike of the Canton Trough at about a 45° angle. Figure 17 is a

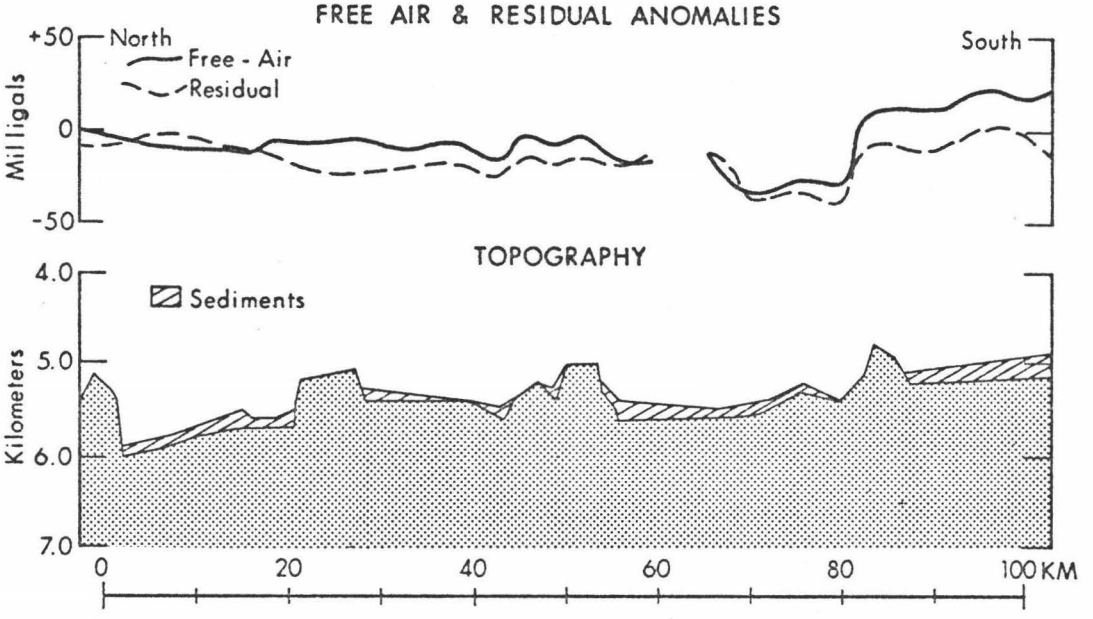

Fig. 17. Gravimetric section MN plotted along a line parallel and equal to section M.

projection of this traverse onto a line roughly equal and parallel to section M. Although spatially correct, the resultant section introduces gravity anomalies having artificial wavelengths. In addition, there are two-dimensional and edge-effect problems which are large enough to invalidate the gravity profiles south of the gap in data. However, it is believed that the remainder of the section is approximately correct. The trend of the residual profile is similar to that shown for section M, although it is displaced towards the negative. Although a model has not been computed, the profile suggests a southward-thickening of the crust.

Section N

This section, shown in Figure 18, is a plot of free-air and residual anomalies. A crustal model is also shown. This section is the topographic equivalent of the southern half of traverse MN. The gravity profiles are probably valid to within 20 km of the southern edge of the section, beyond which they may be too positive because of the nearness of the Phoenix Islands. The residual profile shows a central gravity low similar to that shown for section MN. In the model this low is attributed to a depressed mantle.

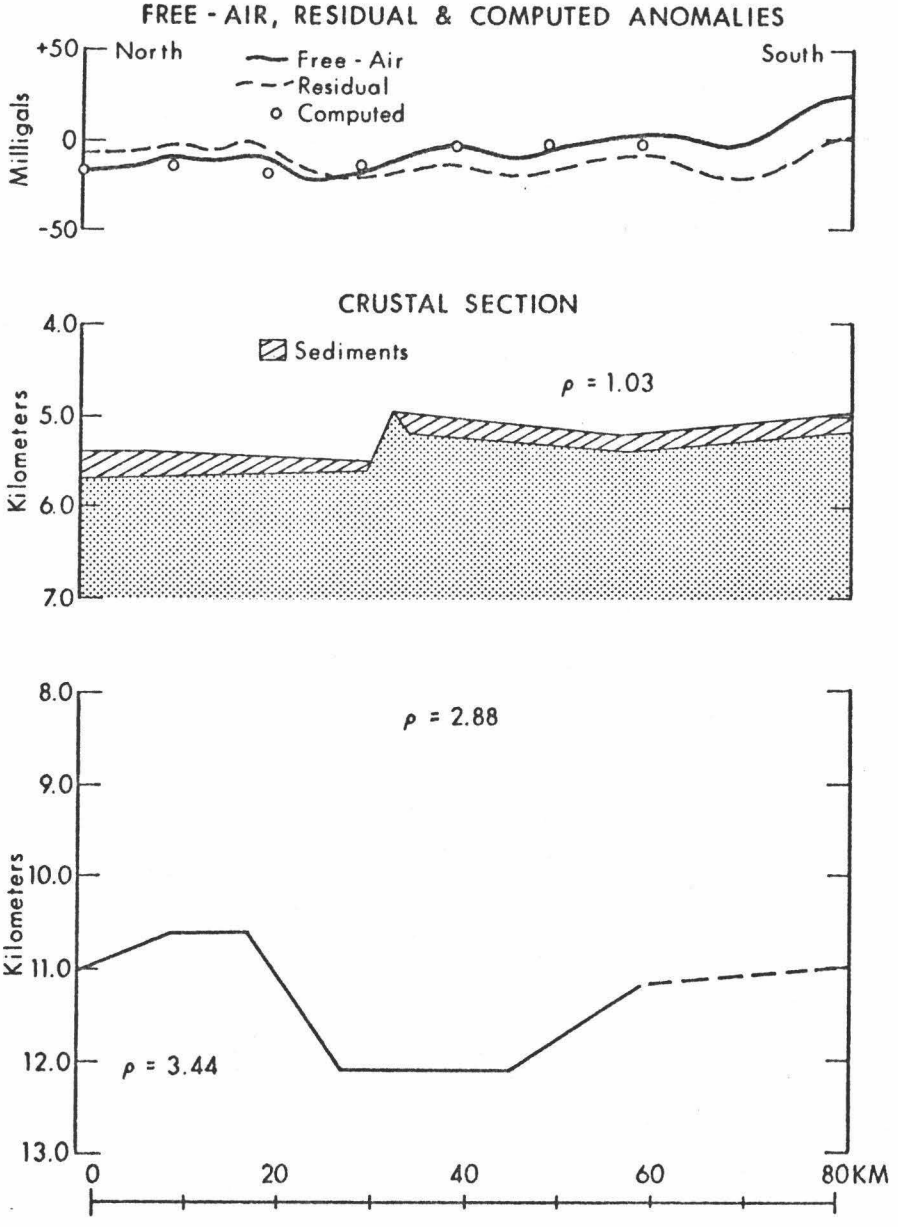

Fig. 18. Gravimetric section N with crustal model.

Regional trends

It is readily apparent that free-air anomalies (Figure 19) generally follow bathymetric lineations (Figure 3). This relationship is especially striking when it is considered that the free-air map is contoured on the basis of significantly fewer data points than is the bathymetry.

Wherever the axial trough is discernible as a distinct bathymetric low, it is characterized by negative free-air anomalies. Where the trough is particularly well developed these anomalies are quite negative, locally exceeding -115 mgals along traverse I in Figure 13. Inside the 7000 m contour, the anomalies are consistently more negative than -60 mgals. At the western end, where the trough apparently disappears (section N), the region is characterized by a general negative free-air anomaly. Negative anomalies also occur over the northeastern part of the region (sections A and B) and are apparently associated with the structural basin (turbidite basin) shown in seismic reflection profile tracings AA' and BB' - CC' (Figure 4) and in Figures 8 and 9. Positive free-air anomalies are associated with the remaining areas; i.e., the northern block-faulted region and the southern ridge and arch between sections E and MN. The southern ridge has anomalies locally exceeding +60 mgals along section H.

Figure 20 shows a contour map of the residual anomalies plotted in sections A through N. It is obvious that the

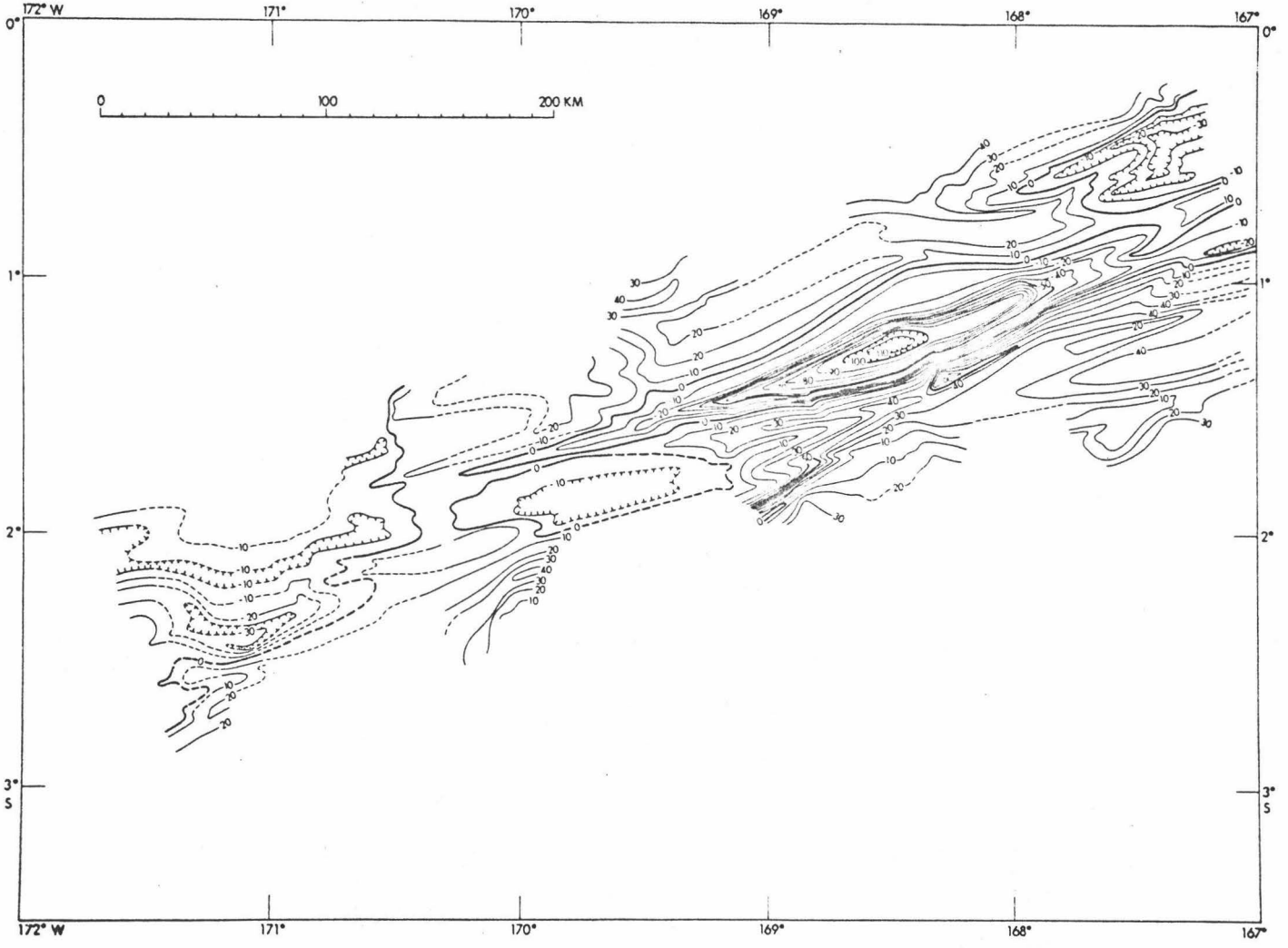

Fig. 19. Free-air anomaly map of the Canton Trough region. Based on gravity stations along ship tracks shown in Figure 7.

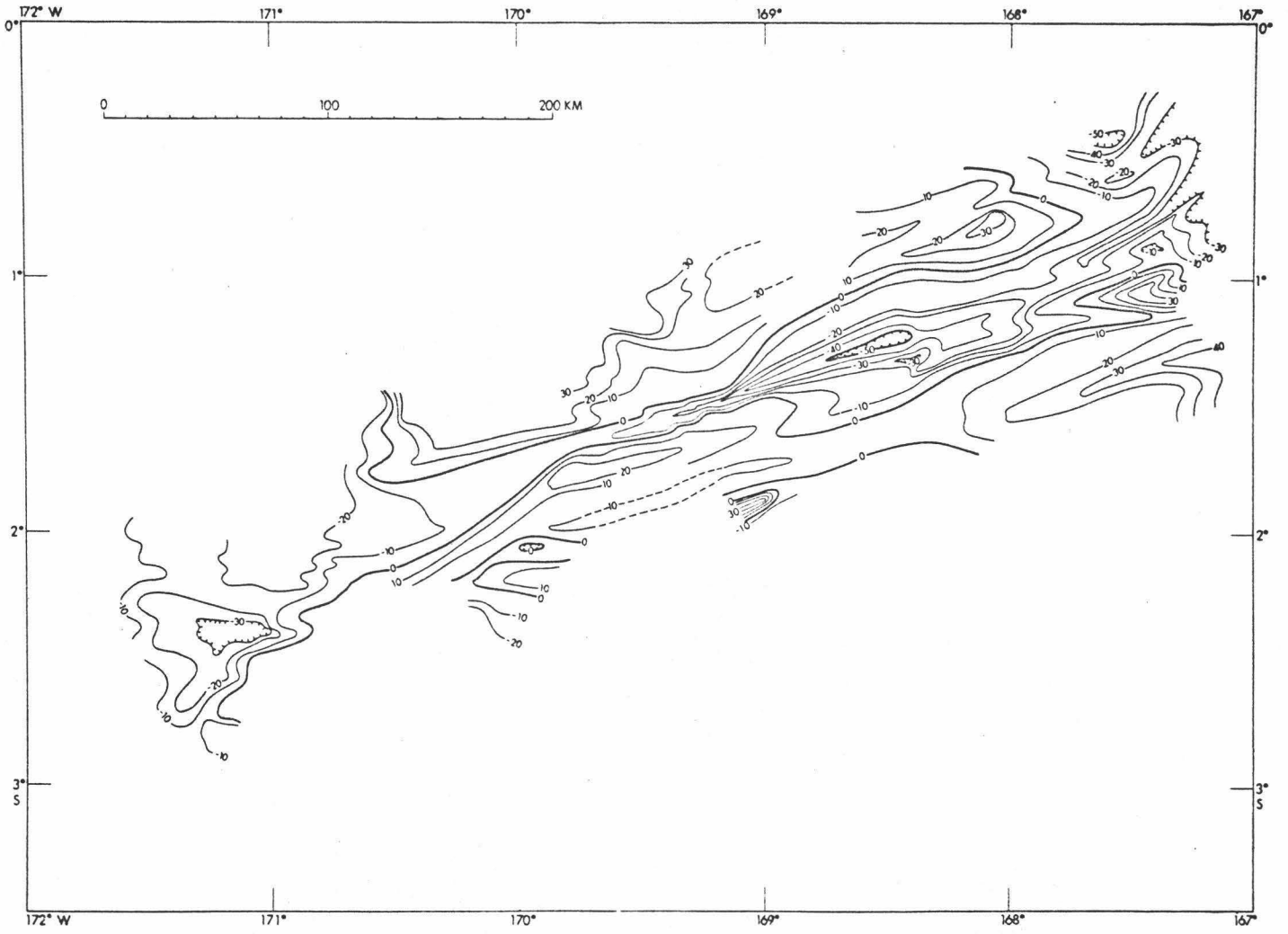

Fig. 20. Residual anomaly map of the Canton Trough region. Based on residual anomaly profiles computed for lettered segments in Figure 7.

residual anomaly map is similar to the free-air map. The major differences are in the absolute values of the anomalies and in the width of the negative band. The negative band is continuous and for the most part follows the ridge-trough system. However, if we consider only those residual anomalies believed to have some geologic significance, the band is probably not continuous, but rather breaks up into two general areas of negative residual anomalies. These areas roughly correspond to the negative parts of the residual anomaly profiles east of section L and west of section M. Between these sections, or between about 169°W and 170°W, the residual anomaly band is too narrow to reflect geologic control. East of 169°W the negative band is quite wide and follows the central volcanic province. On the northeastern end, the band widens indefinitely toward the north. The band also widens west of 170°, and the southwestern end of the Canton Trough is characterized by regional negative anomalies. Positive residual anomalies occur over the remaining areas.

If we compare these geologically controlled residual anomaly patterns to the structure delineated by seismic reflection profiling, there are several outstanding relationships. First, the overall pattern generally follows the trend of the structural lineations, especially between sections B and MN. Second, the anomaly patterns are not necessarily restricted by structural boundaries. Residual

patterns might be expected to transcend some boundaries since the sensitivity of residual anomalies is not high enough to reflect smaller-scale structure. However, anomaly patterns locally transcend the main structural provinces. For instance, both the central volcanic province and the block-faulted region north of it are characterized by negative residual anomalies in sections A and B. In sections E through I the central volcanic province is still characterized by negative anomalies, but the block-faulted region has associated positives. This is also where the central province is topographically well developed.

Apparently, the division of the region into structural provinces is not everywhere consistent with deeper crustal structure. Moreover, if significant variations in crustal structure are indeed reflected in residual anomalies, these variations occur both transverse and parallel to the strike of the Canton Trough. This can be seen by plotting the crust-mantle interfaces computed in sections A through N on a single diagram. This is shown in Figure 21. The interfaces here are aligned with respect to the central trough or its extension.

If we assume that geologically-controlled gravity anomalies result from variations in crustal thicknesses, Figure 21 may indicate that both transverse and parallel variations in crustal structure are systematic. In effect, as the central province becomes more developed towards the

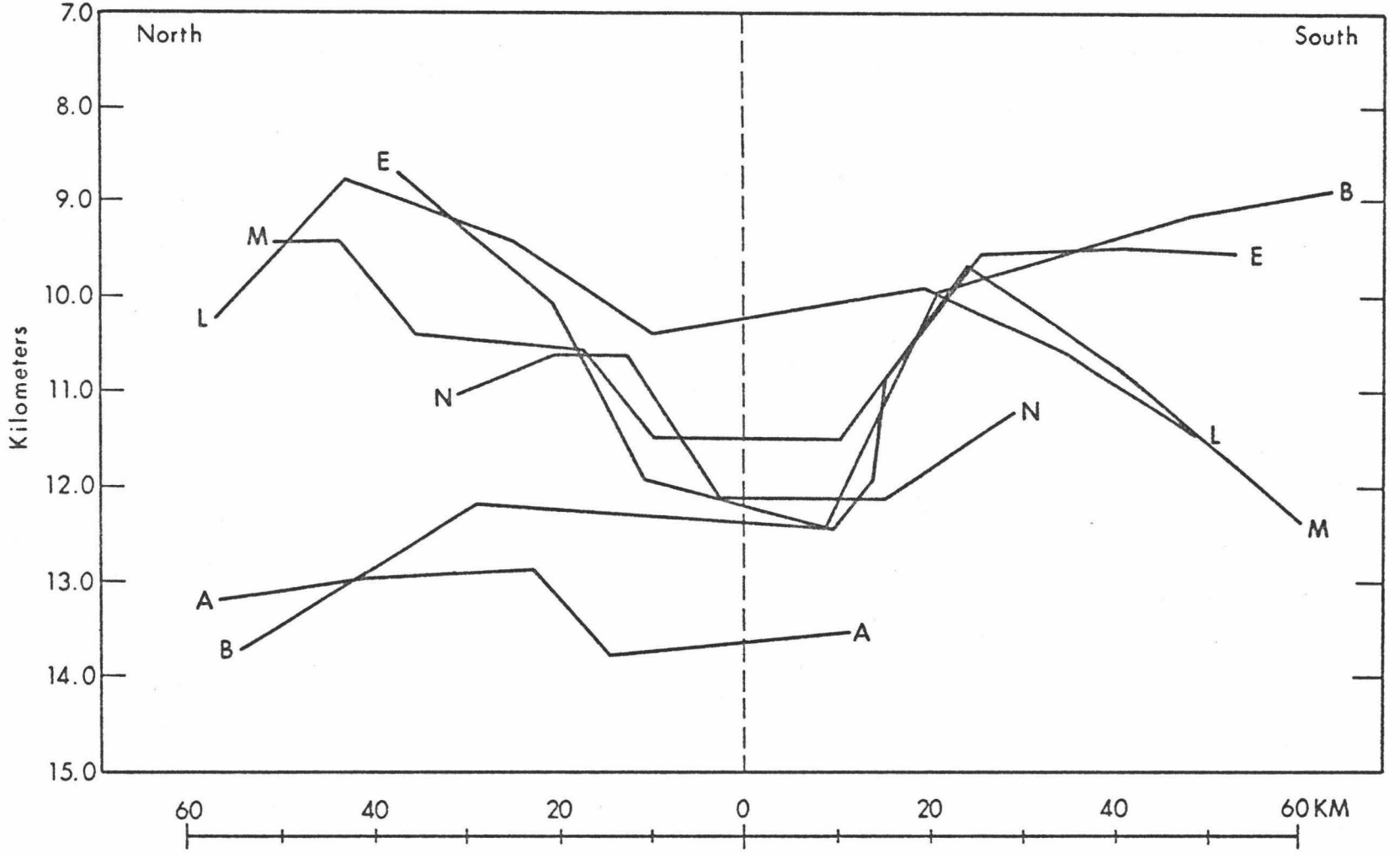

Fig. 21. Crust-mantle boundaries computed for lettered segments in Figure 7. Aligned along axis of the Canton Trough.

west (Figure 4) reaching a maximum in sections E through I, a crustal "root" may be locally developed beneath it. Through the same interval, the crust appears to thin to the north while remaining thin to the south. West of section I the central province becomes subdued (L) and gradually disappears (sections M and N). In conjunction with this, the crust appears to thicken west of section L, but still with the suggestion of a root. It is interesting to note that the characteristic structural patterns associated with the Canton Trough have largely disappeared in the sections west of M, yet there remains a central mass deficiency.

In the above discussion, we assumed that geologically controlled gravity anomalies result from variation in crustal thickness. Alternatively, the anomalies may result from lateral variations in crustal density, possibly related to relatively large intrusions. In this case, the central free-air and residual low may reflect a plutonic body or bodies beneath the central province having a significantly lower density than the surrounding crust. The recovery of plutonic igneous rocks indicates that intrusion has occurred, and the discovery of quartz diorites suggests that the pluton or plutons may, indeed, have a relatively low density. Although difficult to verify, the gravity anomalies probably reflect a combination of variable crustal thicknesses and at least local intrusion.

MAGNETIC STUDIES

Magnetic data were collected during the survey of the Canton Trough region along essentially all ship tracks shown in Figure 2. Shipboard measurements were made using a Varian proton-precession magnetometer. The repetitive response capability of the instrument is excellent, about 2 gammas. However, residual navigation errors of the adjusted track-line crossings indicate that some of the plotted magnetic contours may deviate by as much as 11 gammas.

The work contained herein is preliminary, representing for the most part observations based upon partially reduced data. Although additional study will be included as part of a regional investigation with other authors, the preliminary work is necessarily included here because of its tectonic implications.

Figure 22 shows a map of the total magnetic field for the study area contoured at intervals of 100 gammas. The fundamental pattern here is one of elliptical to extremely elongate bipole anomalies trending parallel to the bathymetric lineations. There is a distinct, narrow belt of anomaly highs, extending from 167° 15'W through 172°W, flanked by negative anomalies.

Although the regional, total-force magnetic field within this area does not greatly mask the anomaly patterns, it has been removed in the residual magnetic anomaly profiles shown in Figure 23. The construction and removal of the regional

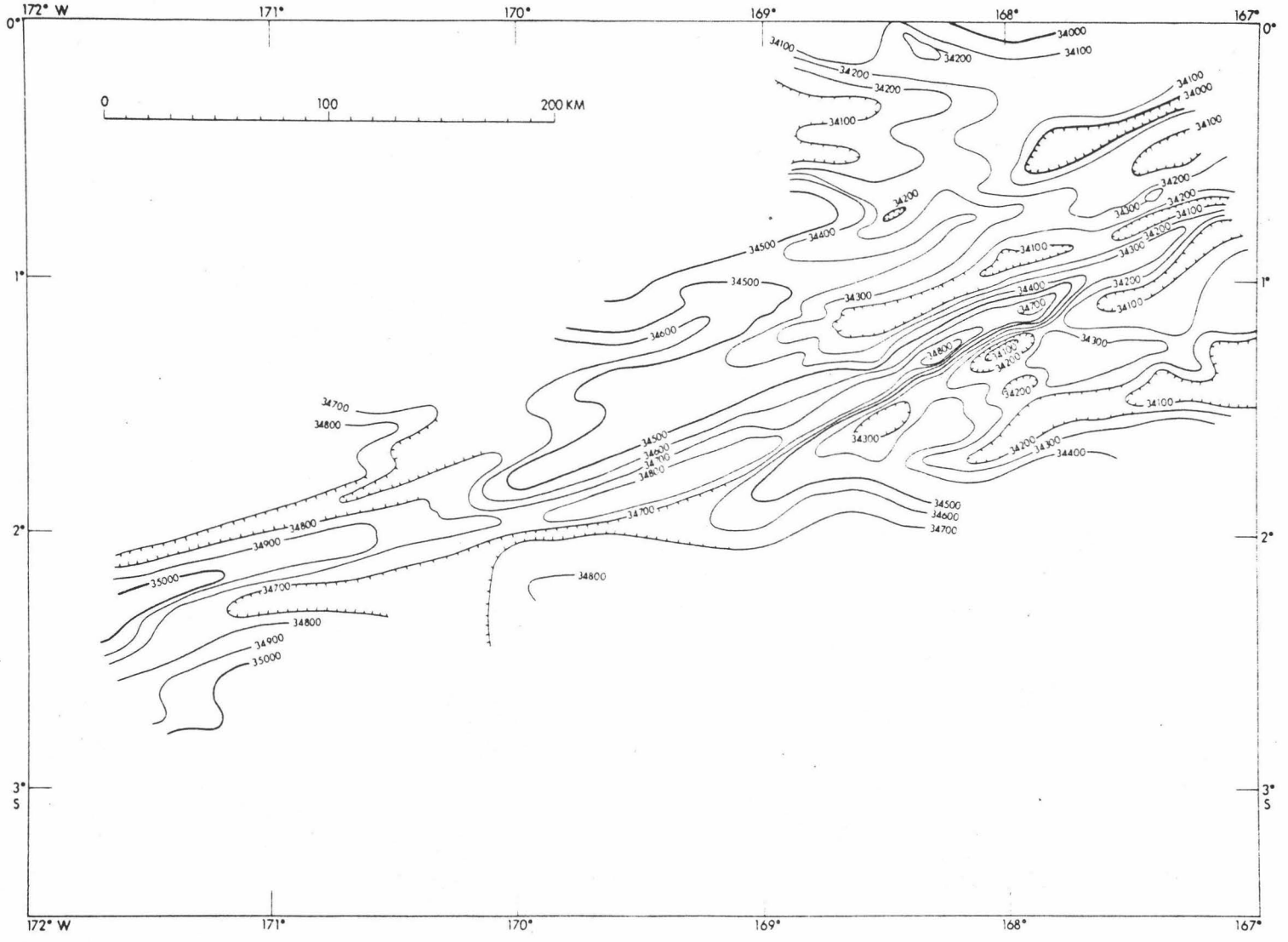

Fig. 22. Total magnetic field contour map for the Canton Trough region. Based on survey data in Figure 2.

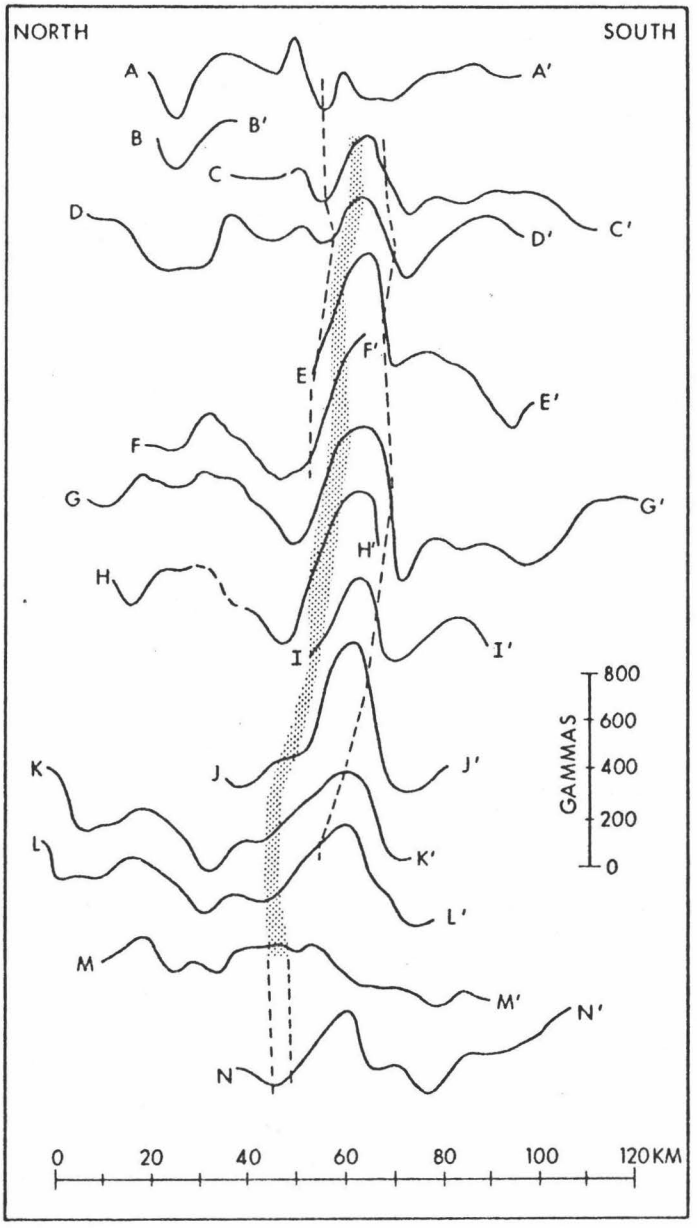

Fig. 23. Residual magnetic anomaly profiles for all lettered traverses in Figure 2. Profiles aligned along central anomaly high or by topographic continuity. Stippled area is the trace of the Canton Trough. Dashed lines are the traces of the northern and southern ridges.

field follows the method described by Malahoff and Woollard [1970]. These workers deduced that since the magnetic field has a source in the outer core of the Earth, it has a smoothly changing function. This function can be constructed by applying least-squares, and smoothing fits to the observed total-force magnetic field.

The residual magnetic profiles are labeled AA' through NN' and are geographically equivalent to similarly labeled seismic reflection profiles (Figure 5) and gravimetric sections (Figures 8 through 18). With the exception of profile AA' and possibly that of MM', all other profiles are aligned with respect to the outstanding central anomaly high. Profiles AA' and MM' are aligned by topographic continuity. The northern and southern ridges and axial deep are also shown where they intersect each signature. It is readily apparent that parts of the magnetic signature can be correlated with topography. From profile AA' through profile JJ', topographic features appear to have a normal polarity for the southern hemisphere and anomaly amplitudes roughly proportional to their development. For instance, within this interval, the pronounced central anomaly high crests over the northern flank of the southern ridge. The peak-to-trough anomaly variations exceed 540 gammas from EE' through JJ', and this is the interval through which topographic relief is most extreme. Maximum relief of magnetic anomalies occurs along profile GG' where the high-to-low variation is about 650 gammas.

Away from the central anomaly pattern and west of profile JJ', the correlation with topography is not as clear. For example, the southern part of the magnetic signatures in profiles DD', EE', and FF' differs substantially, whereas the topography in those profiles is remarkably similar. Also the magnetic signatures of profiles KK' and LL' are like those to the east, but the central high crests south of the southern ridge here. In profile NN', characteristic topographic relief is absent, yet there remains a 320-gamma high aligned with more easterly profiles.

Although continuing work will systematically remove the magnetic-terrain effect of the topography from these profiles, initial approximations (using susceptibility contrasts of the order of 7.5 x 10 cgs units) indicate that a definitive magnetic signature will still be present. In a qualitative sense, the amplitude of the anomaly observed in profile NN' may represent the terrain-corrected anomalies. However, it should be mentioned that petrological and geochemical analyses, discussed in the next section of this work, indicate some of the igneous rocks dredged from this region are extremely rich in magnetite and have unusually high proportions of total iron. Therefore the susceptibility contrast may in reality be considerably higher than that used here.

The above discussion indicates that the magnetic signatures are not entirely generated by the terrain. Therefore, the magnetic anomalies, particularly the central

high, must at least partly reflect a sub-bottom source or sources.

The immediate assumption is that this source is intrusive bodies emplaced during the formation of the Canton Trough and its associated structures. Indeed, the discovery of plutonic rocks is evidence that intrusion has occurred. Also, gravity data indicate a general crustal thickening beneath the central province and local abrupt changes in the depths to Moho. This may be interpreted as evidence for intrusive bodies. Malahoff and Woollard [1970] have used intrusive bodies in the explanation of magnetic anomalies observed along parts of the Murray Fracture Zone. However, to account for the linearity and symmetry of the Canton Trough magnetic signatures, it must be postulated that the intrusions are considerably more linear and regular than surficial structure, and that they cross and even transcend this structure. This is not easily reconciled with a mechanism whereby the emplacement occurs along with the fracturing. Alternatively, the magnetic signatures may be generated by a source unrelated to the surficial structure, implying that the anomalies predate the structure. If this is the case, then the magnetic lineations may be sea-floor spreading anomalies. The linearity, amplitude, and period of the Canton Trough anomalies is comparable to sea-floor spreading anomalies recognized in the northeastern Pacific. Moreover, possible E-W trending sea-floor spreading

lineations have been observed by Larson and Chase [1972] in the vicinity of the Phoenix Islands. These workers have correlated these lineations with NE-SW trending anomalies west of Hawaii and E-W trending anomalies east of Japan [Hayes and Pitman, 1970]. Continuing work should resolve the probable source or sources of the Canton Trough anomalies and should shed some light on their relationship to the lineations described by Larson and Chase.

PETROLOGY AND GEOCHEMISTRY

Rock samples were obtained from the Canton Trough at about 1° 6'S, 167° 56'W, or at the break between profiles EE' and FF' (Figure 2). These samples were inadvertently retained in a piston coring apparatus intended to sample sediments in the axis of the trough. Although the depth here exceeds 7800 m, impact was recorded at about 7100 meters. Apparently the core barrel grazed the lower flank of the southern ridge, collecting several pounds of specimens between 7100 and 7200 meters.

A. Macroscopic descriptions

The rock samples range from sand size to large pebbles. Although many of the samples are quite angular and may be classed as breccia, the majority exhibit at least slight rounding. The rounding and absence of fresh fractures indicates that most of the samples are from talus. Some of the pebbles are highly rounded, superficially resembling those described by Menard [1964] for the Mendocino Ridge. This may be construed as evidence that part of the Canton Trough ridges were at one time above sea level. However, the ridge crests are not truncated indicating a short subareal existence.

The rock specimens show much diversity in their grain sizes, megascopic mineral assemblages, and degrees of

alteration. The majority of the rocks are fine-grained, extensively altered volcanic rocks ranging in color from light brown to gray. A smaller group of specimens are medium- to coarse-grained, fresh to moderately altered plutonic rocks. In several of these rocks, the color indices are well below 40, and primary quartz, amphiboles, feldspar, and magnetite are plainly visible to the unaided eye. In addition, there are also samples of fragile, intact, hollow gas bubbles of fresh volcanic glass and sub-angular to rounded pebbles of friable, glassy cinder, some of which forms a poorly cemented volcanic conglomerate. The glassy cinders are largely unaltered, but fragments of palagonite are occasionally cemented with the pebbles. Three small specimens of "greenstone" were also recovered from this core. These pebbles appear to be chloritized or serpentinized coarse-grained rocks with some opaque minerals still recognizable.

Many of the fine-grained samples are extremely susceptible to magnetic attraction. A small hand magnet will suspend some pebbles as large as one centimeter. Apparently this susceptibility reflects the unusually high content of magnetite found in some samples.

B. Identification and analytical techniques

Thin sections, cut from 34 of the larger rocks, are petrographically described in Table I. Although the sections

TABLE I. PETROGRAPHIC DESCRIPTIONS OF CANTON TROUGH ROCKS

Sample	Rock Name	Petrographic Description
CT-1a	Quartz Diorite	Texture is hypidiomorphic granular; plagioclase laths average 10 mm in length but commonly fractured. 70% calcic andesine; 15% quartz interstitial to andesine; also chlorite, biotite, hornblende, pyroxene (diopside ?), opaques, apatite, pennine, epidote. Section moderately altered; plagioclase partly altered to sericite, chlorite after mafic minerals.
CT-1b	Quartz Diorite	Similar to CT-1a except 50% of section composed of single magnetite grain 20 mm in length.
CT-2a CT-2b	Diorite	Texture is hypidiomorphic granular; plagioclase laths are highly fractured producing stubby subhedral grains that average 8 mm in length. 55-60% andesine; 7-12% hornblende; 5-8% quartz interstitial to andesine; 5% opaques; also chlorite, pyroxene, apatite, epidote (veins). Alteration similar to CT-1a but more variable.
CT-3	Diorite	Texture is hypidiomorphic granular; plagioclase laths fractured producing stubby, subhedral grains, average size of laths about 5 mm. 60% sodic labradorite; 20% hornblende; 5% opaques; also pyroxene, quartz, biotite, chlorite, apatite. Alteration similar to CT-1a.
CT-4	Gabbro	Texture is hypidiomorphic granular; plagioclase laths commonly fractured; average size of laths about 7 mm. 60% andesine; 10% hornblende; also opaques, biotite, chlorite, pyroxene, apatite, pennine, epidote. Extensive alteration of all mineral constituents.

TABLE I. (Continued) PETROGRAPHIC DESCRIPTIONS OF CANTON TROUGH ROCKS

Sample	Rock Name	Petrographic Description
CT-5	Gabbro	Texture is hypidiomorphic granular to diabasic; plagioclase laths stout and subhedral, averaging about 2 mm in length. 50% calcic labradorite; 25% pyroxene; 5% opaques; also hornblende, chlorite, altered biotite, apatite. Alteration of labradorite moderate, of mafics extensive.
CT-6 CT-7	Coarse-grained Diabase	Textures are primarily subophitic; strong preferred orientation of stubby plagioclase laths; average size of laths about 1 mm. 50-60% calcic labradorite (commonly zoned); 15-30% pyroxene; 5-10% opaques; also hornblende, biotite, chlorite. Alteration moderate in CT-6, more extensive in CT-7. Large grains of pyroxene completely altered.
CT-8 CT-9 CT-10 CT-11 CT-12 *CT-13	Extensively Altered Basalt	Textures are primarily diabasic but completely altered interstitial glass also present. Plagioclase laths typically subhedral and often stubby. Average grain size of plagioclase varies from 0.5 mm in CT-9 to 1.0 mm in CT-13. 40-50% labradorite to bytownite; 20-30% pyroxene (probably augite); 10% opaques; 10-15% chlorite. Also small amounts of quartz, olivine, apatite and possibly K-feldspar. Alteration is extreme; plagioclase shows much saussurite and sericite, pyroxene and glass nearly totally altered to iron-stained amorphous clays that give these sections reddish-brown tinge.

*No chemical analysis.

TABLE I. (Continued) PETROGRAPHIC DESCRIPTIONS OF CANTON TROUGH ROCKS

Sample	Rock Name	Petrographic Description
CT-14 CT-15 CT-16 CT-17	Altered Basalt	Textures are primarily diabasic to subophitic. Plagioclase laths typically subhedral, stubby, and corroded. Laths average 0.6 mm in size. 40-50% labradorite; 30-35% pyroxene (augite ?); 5-10% chlorite; 10% opaques. Also olivine, quartz, and possibly K-feldspar. Alteration moderate in CT-14, CT-15, and CT-16, and more extensive in CT-17. Appear to be fresher examples of above group.
CT-18 CT-19 CT-20 CT-21 CT-22	Fine-grained Basalt	Textures are primarily subdiabasic but altered interstitial glass also present. Plagioclase forms both stubby subhedral laths and acicular grains that average 0.3-0.5 mm in length. 40-50% calcic plagioclase; 15-25% pyroxene; 5-15% chlorite; 10% opaques. Also olivine, apatite and vein-filling spherulites and zeolites. Alteration is generally extreme; plagioclase shows much saussurite and pyroxenes badly altered; iron-stained amorphous material gives sections reddish-brown tinge.
CT-23 CT-24 *CT-25	Fine-grained Basalt	Similar to above group but alteration is moderate and grain size of pyroxenes is smaller.
CT-26 CT-27	Fine-grained Basalt	Similar to above group but average grain size of plagioclase about 0.2 mm; alteration moderate and originally more interstitial glass.

*No chemical analysis.

TABLE I. (Continued) PETROGRAPHIC DESCRIPTIONS OF CANTON TROUGH ROCKS

Sample	Rock Name	Petrographic Description
CT-28	Very Fine-grained Basalt	Texture is primarily intersertal, plagioclase microlites < 0.1 mm, matrix of cryptocrystalline material with some pyroxene and much opaque material. Alteration is moderate.
CT-29 CT-30	Porphyritic Basalt	Vesicular, glomeroporphyritic texture; matrix of sub-oriented microlites of labradorite with intergranular altered pyroxene and glass. Also much finely dispersed maghemite. Subhedral phenocrysts of plagioclase largely altered to cherty-like plates; red iron oxides fill interstices between phenocrysts and line fractures and some vesicles; other vesicles partly filled with chalcedony. Alteration is extreme and gives section reddish-brown tinge.
CT-31	Porphyritic Basalt	Glomeroporphyritic texture; matrix of randomly oriented labradorite, microlites, intergranular to sub-ophitic pyroxene, altered glass, and cryptocrystalline material. Also magnetite, maghemite, and chlorite. Stubby, corroded, subhedral phenocrysts of calcic plagioclase; maximum size about 2 mm; some zoning of smaller phenocrysts. Alteration extensive but not as extreme as CT-29; section has greenish-brown tinge.

TABLE I. (Continued) PETROGRAPHIC DESCRIPTIONS OF CANTON TROUGH ROCKS

Sample	Rock Name	Petrographic Description
CT-32	Porphyritic Basalt	Texture is vesicular and porphyritic; microlites of calcic plagioclase and small granules of pyroxene in groundmass of altered glass and crystallites. Phenocrysts of saussuritized calcic plagioclase. Much disseminated opaques. Vesicles filled with chlorite. Alteration is extensive and reddish-brown clays abundant.
CT-33	Porphyritic Basalt	Texture is vesicular and micro-porphyritic; matrix of cryptocrystalline material, altered glass, altered pyroxene. Isolated phenocrysts of altered microlites of plagioclase; iron oxides line fractures and some vesicles. Alteration is nearly complete; section is mostly composed of reddish-brown iron-stained clays.
CT-34	Vesicular Basalt	Texture is vesicular and felted; microlites of randomly oriented plagioclase in groundmass of altered glass and crystallites. Also altered pyroxene and much red iron oxide disseminated throughout section and infilling some vesicles. Vesicles also filled with chalcedony. Alteration is moderate generally and extensive along fractures and vesicles.

are rather diverse in texture, composition, and degree of alteration, many of the sections may still be described in terms of petrographic groups. Some sections are substantially different from the others and merit individual descriptions. The order of the petrographic descriptions in Table I generally follows the grain size of the major mineral constituent or the groundmass. This order also proceeds roughly from intermediate to basic rocks.

Eight of the samples petrographically described in Table I were subjected to X-ray diffraction analyses. These analyses are shown in Table II. The technique used in this study is the diffractometer method described by Klug and Alexander [1954] and Mueller [1967]. Mineralogical identifications have been made from conversion tables provided by Smith [1960, 1964] and Borg and Smith [1969].

Partial chemical analyses (Table III) have been obtained for most of the samples petrographically described and for all samples analyzed by X-ray diffraction. Atomic absorption spectrography was used to determine the major oxides SiO_2, FeO (total iron), MgO, Na_2O, and K_2O, and the trace element Cr. X-ray fluorescence spectrography was used to analyze for TiO_2, Rb, Sr, Zr, Ba, and Ce. The techniques used in the HIG laboratories have been described by Burnett [1971] and Fein [1971] and need not be repeated here. Standards for X-ray fluorescence spectrography have also been discussed by these workers.

TABLE II. X-RAY MINERALOGY OF SELECTED CANTON TROUGH ROCKS

Sample	Rock Name (From Table I)	X-Ray Mineralogy
CT-1	Quartz Diorite	Plagioclase, quartz, magnetite-maghemite, ilmenite, chlorites (prochlorite and kammererite ?), orthopyroxene, pargasite-edenite, montmorillonite.
CT-2	Diorite	Plagioclase, maghemite-magnetite, clinopyroxene, quartz, chlorites, antigorite, trace of hornblende.
CT-6	Diabase	Plagioclase, clinopyroxene, pargasite, hornblende-actinolite, magnetite-maghemite, ilmenite, chlorites, montmorillonite. Possibly anthopyllite, edenite. Unidentified strong peaks at 2.13 and 2.14Å.
CT-9	Basalt	Plagioclase, magnetite-maghemite, clinopyroxene (probably augite), quartz, chlorites, montmorillonite.
CT-14	Basalt	Plagioclase, clinopyroxene (probably augite); minor maghemite-magnetite, quartz, monoclinic amphiboles (actinolite-tremolite, edenite), ilmenite. Strong unidentified peak at 4.11Å.
CT-18	Fine-grained Basalt	Plagioclase, clinopyroxene, magnetite-maghemite, quartz, trace of chlorite. Sample does not yield good X-ray patterns.
CT-23	Fine-grained Basalt	Plagioclase, clinopyroxene, magnetite-maghemite, chlorite. Possibly enstatite, olivine and apatite.
CT-28	Very fine-grained Basalt	Plagioclase, clinopyroxene, magnetite-maghemite, quartz. Possibly apatite and dioctahedral micas. Sample does not yield good X-ray patterns.

TABLE III. PARTIAL CHEMICAL ANALYSES OF CANTON TROUGH ROCKS

	CT-1	CT-2	CT-3	CT-4	CT-5	CT-6	CT-7
TiO_2	1.25	0.48			0.88		
FeO*	14.41	10.68	10.86	11.99	8.16	8.20	10.04
MgO	5.56	5.89	4.80	3.54	3.99	8.71	10.31
Na_2O	2.59	4.55	3.01	4.03	3.85	1.80	2.38
K_2O	0.18	0.23	0.31	1.10	0.55	0.46	0.40
Cr	38	90	57	15	50	69	85
Rb		17			16		
Sr	104	180			150		
Zr	103	58			170		
Ba	56	55			23		
Ce	76	45			95		
Na_2O+K_2O	2.77	4.78	3.32	5.13	4.40	2.26	2.78
Na_2O/K_2O	14.39	19.78	9.70	3.66	7.00	3.15	3.56
FeO*/MgO	2.59	1.81	2.26	3.39	2.04	0.94	0.97
K_2O/Rb		135			344		
Sr/Rb		10.59			9.38		

*Total iron.

TABLE III. (Continued) PARTIAL CHEMICAL ANALYSES OF CANTON TROUGH ROCKS

	CT-8	CT-9	CT-10	CT-11	CT-12
TiO_2	1.76	1.63			
FeO*	14.84	14.60	14.51	14.02	
MgO	2.70	4.24	4.06	3.59	4.34
Na_2O		3.02	3.63	4.99	3.35
K_2O	1.30	1.19	0.98	0.51	0.94
Cr	152	173	195	163	145
Rb	24	23			
Sr	104	103			
Zr	180	137			
Ba	39	46			
Ce	114	118			
Na_2O+K_2O		4.21	4.61	5.50	3.29
Na_2O/K_2O		2.54	3.70	9.78	3.56
FeO*/MgO	5.50	3.44	3.57	3.90	
K_2O/Rb	541	517			
Sr/Rb	4.33	4.48			

*Total iron.

TABLE III. (Continued) PARTIAL CHEMICAL ANALYSES OF CANTON TROUGH ROCKS

	CT-14	CT-15	CT-16	CT-17	CT-18
TiO_2	1.77	1.06			3.35
FeO*	10.36	11.76	10.63	11.45	15.19
MgO	6.50	6.89	5.93	5.81	3.21
Na_2O	3.92	3.64	3.55	4.28	4.43
K_2O	0.41	1.06	0.18	1.36	0.66
Cr	166	161	188	387	156
Rb	14	15			30
Sr	111	107			106
Zr	135	140			220
Ba	81	26			94
Ce	47	116			121
Na_2O+K_2O	4.33	4.70	3.78	5.64	5.09
Na_2O/K_2O	9.56	3.43	19.72	3.15	6.71
FeO*/MgO	1.59	1.71	1.79	1.97	4.73
K_2O/Rb	293	707			220
Sr/Rb	7.93	7.13			3.53

*Total iron.

TABLE III. (Continued) PARTIAL CHEMICAL ANALYSES OF CANTON TROUGH ROCKS

	CT-19	CT-20	CT-21	CT-22	CT-23
TiO_2	1.34				2.03
FeO*	12.51	12.69	13.71	13.75	13.16
MgO	4.67	5.39	5.10	5.06	6.28
Na_2O	3.28	4.31	8.78	3.06	3.10
K_2O	1.12	1.21	0.83	0.63	0.35
Cr	108	196	247	129	107
Rb	30				
Sr	131				120
Zr	125				143
Ba	35	76			109
Ce	87	74			55
Na_2O+K_2O	4.40	5.52	9.61	3.69	3.45
Na_2O/K_2O	2.93	3.56	10.58	4.86	8.86
FeO*/MgO	2.68	2.35	2.69	2.72	2.09
K_2O/Rb	373				
Sr/Rb	4.37				

*Total iron.

TABLE III. (Continued) PARTIAL CHEMICAL ANALYSES OF CANTON TROUGH ROCKS

	CT-24	CT-26	CT-27	CT-28	CT-29
TiO_2					
FeO*	12.05	13.47	9.49	14.75	12.83
MgO	6.51	5.85	7.23	2.28	3.53
Na_2O	2.87	3.78	3.04	2.27	4.43
K_2O	0.21	0.55	0.75	0.17	1.85
Cr	173	138	314	7	267
Rb					
Sr					
Zr					
Ba					67
Ce					97
Na_2O+K_2O	3.08	4.33	3.79	2.44	6.28
Na_2O/K_2O	13.67	6.87	4.05	13.35	2.39
FeO*/MgO	1.85	2.30	1.31	6.47	3.63

*Total iron.

TABLE III. (Continued) PARTIAL CHEMICAL ANALYSES OF CANTON TROUGH ROCKS

	CT-30	CT-31	CT-32	CT-33	CT-34
TiO_2					
FeO*	11.53		10.81	12.57	17.31
MgO	1.90	6.68	6.12	7.20	4.46
Na_2O	3.63	2.61	3.06	3.28	4.19
K_2O	1.96	0.85	0.98	0.73	1.34
Cr	256	117	255	50	62
Rb					
Sr					
Zr					
Ba					166
Ce					74
Na_2O+K_2O	5.59	3.46	4.04	3.69	5.53
Na_2O/K_2O	1.85	3.07	3.12	4.49	3.13
FeO*/MgO	6.07		1.77	1.74	3.88

*Total iron.

In order to evaluate the precision of the atomic absorption measurements, replicates of samples CT-1, CT-5, CT-10, CT-17, CT-19, and CT-31 were made and analyzed at various times during the course of this work. The values of these replicates are shown in Table IV. SiO_2 is a difficult element to determine by rapid techniques and it is apparent that SiO_2 values so determined are inadequate with respect to the desired precision. This is largely attributed to the highly refractory nature of this element in atomic absorption flames. To increase the precision of SiO_2 determinations, X.R.F. spectrography was employed, but relatively large particle size and the unavailability of an appropriate target tube invalidated the measurements (W. C. Burnett, personal communication). Therefore, SiO_2 values are not reported in Table III. Also, Na_2O replicates of sample CT-1 vary substantially. This probably reflects contamination by sub-standard de-ionized water used in the preparation of this one sample (this problem did not apply to other samples). Although other Na_2O replicates are fairly good, some values in Table III are suspiciously high. These high values should be used with caution. The remainder of the determinations, especially FeO, MgO, and K_2O, have a precision suitable for the requirements of this study. The relatively large sample-size required for X-ray flourescence spectrography did not permit replicate analyses of this method. The precision of this method as employed in

TABLE IV. DATA ON REPLICATE RUNS OF SIX SAMPLES FROM THIS STUDY

Sample		SiO_2	*FeO	MgO	Na_2O	K_2O	Cr (ppm)
	a	51.19	10.68	6.47	4.11	0.45	176
	b	45.25	10.45	6.37	2.79	0.35	163
1	c	46.63	10.13	6.28	2.96	0.35	168
	d	40.62	10.19	6.86	5.80	0.48	132
	a					0.64	
5	b					0.69	
	a	49.38	11.63	3.53	4.12	1.00	16
	b	50.03	11.96	3.49	4.00	1.13	14
10	c	49.16	12.59	3.65	3.93	1.06	14
	d	49.56	11.78	3.51	4.07	1.20	16
	a	46.85	10.59	5.86	3.55	0.18	177
17	b	50.84	10.65	6.01	3.55	0.19	202
	c	45.98	10.64	5.91	3.56	0.18	184

TABLE IV. (Continued) DATA ON REPLICATE RUNS OF SIX SAMPLES FROM THIS STUDY

Sample	SiO_2	*FeO	MgO	Na_2O	K_2O	Cr (ppm)
19 a	50.92				0.85	
19 b	50.08				0.84	
31 a					0.40	
31 b					0.39	

*Reported as total iron.

the HIG laboratories has been discussed by Burnett [1971] and Fein [1971], and in the evaluation of the analyses by X.R.F. in this study, the same precision has been assumed.

C. Discussion

Medium- and coarse-grained samples

The petrographic descriptions in Table I indicate that samples CT-1 through CT-7 are plutonic rocks ranging in composition from quartz diorite to gabbros and diabases. Several small hand specimens, not sectioned, show as much as 40% quartz, and therefore the range may extend to rocks even more silicic than quartz diorite. It is somewhat unrealistic to assign names to pebble-size samples and coarse-grained thin sections from such samples, but the small size of most specimens in this study made this situation unavoidable.

With few exceptions [Miyashiro et al., 1969a; Aumento, 1969; and Fox et al., 1971], oceanic plutonic rocks of intermediate to acid composition are not considered indigenous to oceanic crust [Aumento, 1969; Aumento and Loncarevic, 1969]. When such rocks are found on the ocean floor they are usually attributed to an erratic origin; principally ice rafting during the Pleistocene epoch. Aumento [1969] and Aumento and Loncarevic [1969] have listed diversity, roundness, striations, and lack of ferromanganese coatings as indicators for ice-rafted erratics. The Canton Trough rocks

are certainly diverse in composition, but since it is likely that a talus slope was sampled, at least some diversity would be expected. Further, although many Canton Trough rocks are rounded, the plutonic samples are mostly subangular. Striations are not evident on any sample. Ferromanganese coatings are generally lacking, but this is not necessarily an indicator of recent ice-rafting. The environment may not be favorable for manganese accretion. Also, faulting may have exposed these rocks recently. The alteration of these rocks suggests an environment low in oxygen (G. A. Macdonald, personal communication) and consequently unfavorable for deep-sea manganese accretion. It would seem, therefore, that any attempt to build a case for the erratic origin (by ice) of the more silicic plutonic rocks from the Canton Trough, 100 km from the equator, must be based solely on their unusual mineralogy, which is atypical for any ocean basin.

Transport mechanisms other than ice may account for the presence of the intermediate plutonic rocks. These include organic transportation [Emery, 1963] and turbidity currents. Organic transportation is statistically unlikely for this region, but turbidity currents are believed to play an important role in sediment distribution within the Canton Trough region. However, it has been previously stated that the axial deep is closed to turbidite plumes and therefore transport of the rocks by this mechanism is highly unlikely.

Although the problem of whether the quartz diorites and diorites are erratic or indigeneous cannot be solved on the basis of a small single "dredge" haul, several factors should be considered. Foremost is an apparent petrographic gradation from the basic plutonic rocks to those of intermediate composition. In particular, textures become coarser grained, quartz becomes prevalent, plagioclase becomes more sodic, more euhedral, and less equant, and amphiboles increase in abundance. Moreover, rather large grains of magnetite are found in these plutonic rocks (see CT-1b description). Their occurrence in the more basic members is not unexpected, but in diorites and quartz diorites formed from large bodies of intermediate to silicic magmas, their presence would be quite unusual. These observations suggest locally advancing fractionation as a mode of origin of the more silicic plutonic rocks. However, the chemical analyses of CT-1 through CT-7 (Table III) do not exhibit any trends indicative of fractionation. Since SiO_2 values are unreliable, this oxide cannot be used in any variation diagram illustrative of differentiation processes. Alternatively a MgO - FeO - (Na_2O + K_2O) diagram is shown in Figure 24 for these samples, but again, there is no strong evidence of fractionation.

In view of the incomplete nature of the analyses, the degree of alteration, and the large analytical errors displayed by SiO_2 and probably Na_2O analyses in this study,

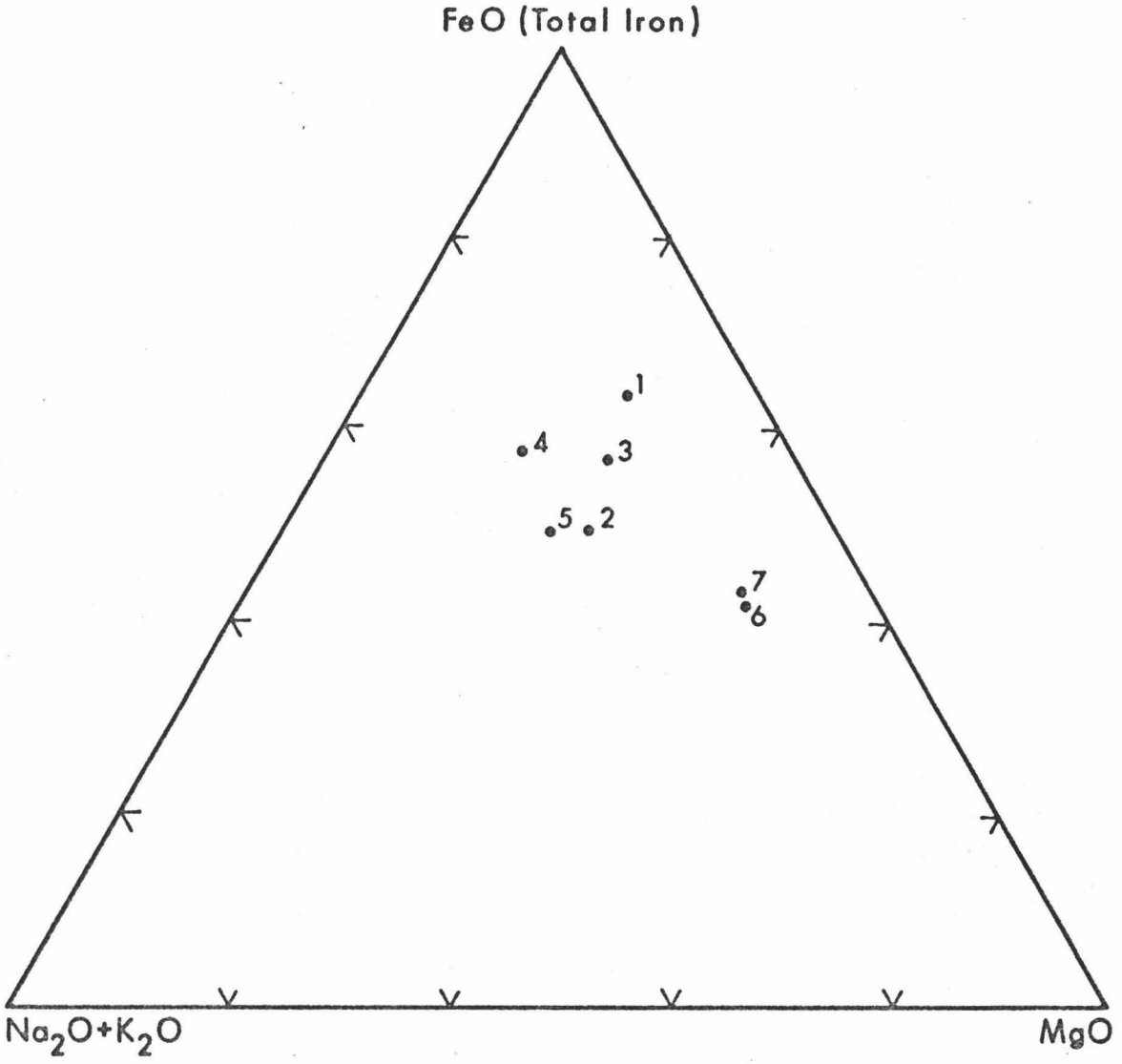

Fig. 24. MgO-FeO-(Na_2O+K_2O) diagram for medium and coarse-grained intrusive rocks from the Canton Trough. Numbers here and in Figure 25 refer to samples listed in Tables I, II, and III.

too much weight should not be given to the chemical data. The author therefore presently favors a mode of origin for the more silicic plutonic rocks by differentiation from a parent basaltic magma. If these rocks are indeed "in situ" samples, then magmatic differentiation must have progressed much further than usually thought possible within the oceanic crust. The occurrence of granitic rocks within the Canton Trough may be analagous to their discovery on the Aves ridge [Fox et al., 1971].

Fine-grained samples

Samples CT-8 through CT-34 are fine-grained volcanic rocks petrographically identified as basalts. Textures are variable, ranging from diabasic and ophitic to intersertal, glomeroporphyritic, porphyritic, and vesicular. Alteration is always evident, but differs substantially in its intensity.

The large analytical uncertainty of the SiO_2 values and the questionable Na_2O determinations make it difficult to separate the igneous rocks from the Canton Trough into tholeiitic and alkalic suites on the basis of diagrams of total alkalis versus SiO_2 [Macdonald and Katsura, 1964] or K_2O versus SiO_2 [Engel et al., 1965]. Indeed, the identification of these samples as basalt cannot even be chemically confirmed! In view of these difficulties it would be judicious to point out that the following discussion is very tentative.

Many workers [Engel and Engel, 1964, 1965, 1970; Engel et al., 1965; Gast, 1968; Kay et al., 1970; Miyashiro et al., 1969a, 1969b; Philpotts et al., 1969; and Tatsumoto et al., 1965] have proposed that oceanic tholeiites are characterized by particular concentrations of certain elements and oxides. With respect to the chemical analyses presented here, unaltered oceanic tholeiites should have distinctly low concentrations of K_2O, Ba, Sr, and Zr. They also should have ratios of FeO (total iron)/MgO of 0.76 - 1.85, $Na_2O/K_2O > 10$, K_2O/Rb of about 1300, and Sr/Rb of about 130. If it is assumed that the petrographic identifications of these specimens are correct, i.e., that they are basalts, then these characteristics can be applied to Canton Trough volcanic rocks to determine their tholeiitic or alkalic tendencies. Before applying these parameters to Canton Trough rocks however, the effects of sea water alteration on the concentrations of many of these elements and oxides must be at least qualitatively examined.

The relative change in elemental abundances with progressive sea water alteration can be partially assessed by comparing the mineralogy and chemistry of group samples CT-8 through CT-13 and CT-14 through CT-17. On the basis of petrographic studies it is believed that group CT-8 through CT-13 is composed of highly altered variations of the group CT-14 through CT-17. Comparing the chemical analyses of these groups in Table III, it is apparent that the highly

altered specimens (CT-8 through CT-13) are distinctly enriched in total iron and depleted in MgO. The FeO/MgO ratios reflect this variance rather well, tending to increase with alteration. Therefore this ratio may not be indicative of the primary tholeiitic or alkalic natures of highly altered oceanic basalts.

Na_2O values, although variable, do not indicate significant systematic changes between these grades of alteration. If Na_2O concentrations vary during alteration, the change presumably occurred at earlier stages of alteration. Also Sr values, although partially lacking, do not suggest significant variations. Rb may increase slightly from the moderately altered to highly altered groups, but Sr/Rb ratios are much less than 130 for both groups. Ba and Zr concentrations are inconclusive.

K_2O concentrations show fluctuations within the two groups that are as large as those between the groups. This suggests that if K_2O values change at comparable rates (for similar rocks) during sea water alteration, the original K_2O concentrations of rocks within these groups must have been substantially different.

Hart and Nalwalk [1970] and Philpotts et al. [1969] studied sea water alteration of submarine basalts and have concluded that alteration can produce very large increases in Rb concentrations, sizable increases in K_2O concentrations (2 to 5 times original values), moderate increases or

decreases in Ba concentrations, and little or no significant changes in Sr values. From these conclusions and the observations presented here, it would appear that Rb, K_2O, and Ba concentrations and FeO/MgO, K_2O/Rb, Sr/Rb, and Na_2O/K_2O ratios should be used with care in interpretations involving altered submarine basalts. In effect, extensive alteration of tholeiitic basalts may yield rocks with many of the chemical characteristics of alkalic basalts. Therefore altered basalts having oceanic tholeiitic affinities were probably originally tholeiitic.

Using K_2O concentration as the criterion for distinguishing tholeiitic basalts from other types, samples CT-16, CT-24, and CT-28 have values within the ranges reported for average oceanic tholeiitic basalt [Engel et al., 1965]. In addition, Na_2O values are comparable to the average tholeiite. Other elemental and oxide concentrations for these samples seem to show some effects of alteration and tend to fall between the values for average tholeiite and average alkalic basalt. Assuming the maximum enrichment of K_2O content, caused by seawater alteration, to be five times the original concentration [Hart and Nalwalk, 1970], the highly altered basalts presently found having K_2O values exceeding about 1.10 weight per cent cannot be normal oceanic tholeiites. Samples CT-8, CT-9, CT-17, CT-19, CT-20, CT-29, CT-30, and CT-34 fall within this category. Most of these samples show chemical characteristics more compatible with alkalic basalts than

with tholeiitic basalts. Even considering the extensive alteration, these samples were probably not originally tholeiitic. The remainder of the samples have intermediate values of K_2O and rather variable concentrations of other elements and oxides. Several of these have probably lost their original tholeiitic characteristics due to alteration, but the majority may have already been intermediate between the tholeiitic and alkalic suites prior to alteration changes.

From the above chemical evidence, Canton Trough basalts appear to represent members of the tholeiitic, transitional, and possibly alkalic suites as defined by Engel et al. [1965]. However, petrographic evidence for a higher degree of oxidation of the samples with chemical alkalic tendencies is not observed. For instance, comparing the descriptions in Table II of the very low potassium samples (CT-16, CT-24, CT-28) with some of the high potassium samples, it is apparent that hornblendes (oxy-hornblendes), titanium oxides, magnetite, maghemite, and ilmenite do not increase in abundance in the high-potassium samples. Indeed, CT-16 (low K_2O) and CT-17 (high K_2O) are almost petrographically identical. Miyashiro et al. [1969b] have also noted considerable chemical variations for similar thin sections and hand specimens of abyssal (oceanic) tholeiites. It should be noted that the basalts with porphyritic and vesicular textures tend to have higher average values of K_2O than other basalts. If Canton

Trough basalts include members of the above suites, petrographic differences are apparently masked by the effects of extensive alteration.

Many workers believe that the transitional and alkalic basalts are derived from a parent tholeiitic magma, and numerous plots and diagrams have been employed to illustrate fractionation trends. Canton Trough basalts were plotted on the more common diagrams used to show differentiation processes, but trends either do not exist or are largely masked by alteration effects. For instance, Figure 25 is an A-F-M diagram for volcanic rocks from the Canton Trough. Although a band along the tholeiitic trend may exist, the scatter is extreme. Combining Figures 24 and 25 enhances the trend, but because of the enrichment in total FeO and depletion in MgO with progressive alteration and the unusually high concentration of Na_2O in some samples, the genetic significance of these plots is questionable.

Engel and Engel [1970] have reported tholeiitic basalts and gabbros from the scarp of the "Argo Trench." Since this trench is probably part of the Canton Trough, as previously mentioned, the data presented here indicate that crustal rocks within this region may be considerably more diverse than reported by these workers. Engel and Engel [1970] have also reported equivocal ages of over 75 million years for some of the tholeiites and gabbros. The fresh volcanic glass bubbles and glassy cinders reported in this study

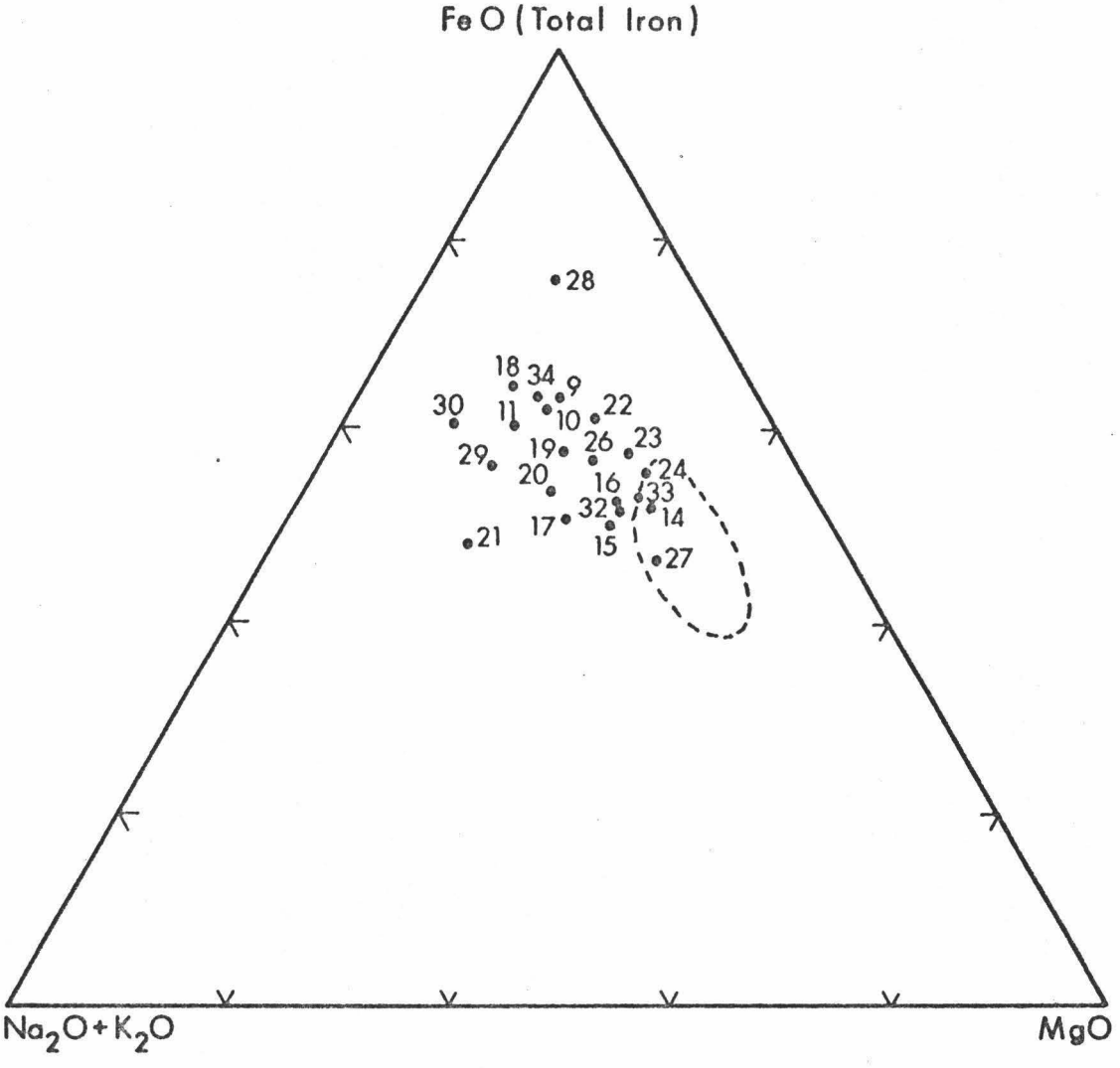

Fig. 25. MgO-FeO-(Na_2O+K_2O) diagram for fine-grained basalts from the Canton Trough. The outlined field encloses range for abyssal (oceanic) tholeiites from mid-ocean ridges [Miyashiro et al., 1969].

strongly indicate that relatively recent volcanism has also occurred. Moreover, both altered and fresh fragments of intermediate plutonic rocks were recovered. If these fragments are not erratic, the various stages of alteration indicate that either faulting or intrusion have occurred at various times within the region.

TECTONIC PROCESSES

The earlier sections of this work have been primarily limited to the presentation and analysis of data within the surveyed region. To evaluate tectonic processes involved in the formation of the Canton Trough, we next must determine the spatial extent of this feature.

Extensive faulting is not observed south of the aforementioned arch-like feature (Figures 5 and 6 IV) and the region there forms a rather wide basin on easterly crossings. Although R/V MAHI survey data are incomplete and data from other sources are unavailable, tectonic processes associated with the formation of Canton Trough structures probably do not involve crust south of this arch.

There is evidence that the northern province may continue much farther north than is known from R/V MAHI data above. Ewing et al. [1968], and Ewing and Ewing [1970, Figure 47] show a reflection profile near the equator at 170°W which contains several isolated structures that appear fault-bounded. Menard [1964, 1967] depicts several troughs and ridges, nearly parallel to the Canton Trough, that are at least 800 km north of the Trough. Chase et al. [1970] also illustrate several topographic highs and three regions where depths approach 6000 m in the area between 166°W and 170°W, and between the equator and 5°N. Moreover, seismic reflection record 103 from Leg VII of the D.S.D.P., located at about 169°W and 3°N, shows a possible upfaulted block, but other

reflection records in this region from Leg VII do not suggest faulted topography [Kroenke et al., 1971]. However, this segment of Leg VII parallels the strike of the Canton Trough, and so may have missed most E-W trending structures.

The above observations indicate that faulted structures may persist for considerable distances north of the equator, although faulting may not be as intense as in Figure 6 I. Therefore the northern province is probably much wider than its surveyed width of 100 km, implying that the tectonic processes responsible for the formation of the Canton Trough involve a substantial section of the Central Pacific Basin.

In addition to the northern continuation, the Canton Trough and its associated structures form a zone that probably is much longer than indicated by R/V MAHI data. Although bathymetric expression within the zone is not clearly observed west of traverse MN' (Figure 2), the magnetic and gravity data suggest a continuation through profile NN', just east of the Phoenix Islands. However, there are no obvious bathymetrical, structural, or magnetical disruptions to indicate that the zone continues through the Phoenix Islands. This implies that the zone disappears beneath the archipelagic apron of the Phoenix Islands, analagous to the disappearance of the Molokai fracture zone within the Hawaiian archipelago and its reappearance to the west [Malahoff et al., 1966]. Alternatively, the zone may actually terminate by splaying or branching [Menard, 1967]

east of Canton Island. Unfortunately, data immediately west of the Phoenix group along the W-SW trend of the Trough have not been collected. The 7300-m deep described by Menard [1967] is certainly part of the Canton Trough, but Menard believes this deep is part of a zone that continues west along the northern edge of the Phoenix Islands. This indicates a possible westward continuation of the Canton Trough zone or a branch of it, in an en échelon fashion.

Menard [1967] and Engel and Engel [1970] have concluded that the east-northeast trending lineations west of the Line Islands, which include the Canton Trough zone, are the extension of the Clipperton fracture zone into the Central Pacific Basin. Several lines of evidence from data presented in this work support this contention. Foremost is the near coincidence of the extensions of these features. The eastward extrapolation of the strike of the Canton Trough (here taken as the average trend of the central province) intersects the Line Islands only 180 km north of where the western end of the Clipperton fracture zone intersects these islands. Since the strikes of the Canton Trough and Clipperton fracture zone differ by only about 4°, a slight change in strike of the eastward extension of the Canton Trough could easily align the features. Unfortunately, data between the surveyed region and the Line Islands are incomplete and thus bathymetric continuity within this region cannot be firmly established. However, Chase et al. [1970] depict vaguely

aligned ridges and troughs parallel to and south of the eastward extension of the Trough's strike. These features suggest intermittent continuity as far as the western edge of the Line Islands' archipelagic apron. Furthermore, the large graben north of the axial deep (Figure 6 II, 6 III) forms a basin for turbidite deposition from the east-northeast. This indicates structural continuity as far east as the turbidite source, which is believed to be the Line Islands. Also, Malahoff (personal communication) has noted disturbed magnetic lineations along the western edge of the Line Islands' apron that may be associated with the reappearance of the Clipperton zone west of that island group. Again, structural continuity is indicated.

In addition to the close alignment of the extensions of the Canton Trough and Clipperton fracture zone, the features are somewhat similar in geomorphology. Menard and Chase [1970] have described the topography, linearity, and trend associated with fracture zones. With respect to these parameters, the Canton Trough differs from the Clipperton fracture zone only in its extreme relief and depths. However, extreme depths are not unknown for fracture zones, as exemplified by the 7728 m Romanche Trench, which is part of the Romanche fracture zone [Heezen et al., 1964]. Therefore, the Canton Trough and its associated structures may continue eastward to the Line Islands forming a Central Pacific segment of the Clipperton fracture zone. If this is the case

then the mechanisms involved in the formation of the Canton Trough zone are simply those responsible for the formation of major North Pacific fracture zones.

Menard and Atwater [1968] and Menard and Chase [1970] have proposed models for fracture zone generation that are readily applicable to the Canton Trough. The basic tenents of these models are: (1) that fracture zone topography is produced at mid-ocean ridges by active ridge-ridge transform faults [Wilson, 1965] and preserved intact along inactive segments (fracture zones); and (2) lateral variations in fracture zone topography and trend may result from changes in sea-floor spreading direction through time. Specific application to the Canton Trough requires a reorientation of spreading centers at the East Pacific Rise at the time in which the change in trend occurs between the western end of the Clipperton fracture zone and eastern end of the Canton Trough. Thus the age of the oceanic crust in the vicinity of where the Clipperton trend changes to the Canton Trough trend should coincide with the time of formation of the Trough. From JOIDES drilling in the Central Pacific Basin during Leg VII [Winterer et al., 1971], basement in this region is probably of Late Cretaceous age. This correlates well with the 70-million-year ages Engel and Engel [1970] arrived at for "Argo Trench" tholeiitic basalts and gabbros.

The mode of adjustment of the ridge-ridge transform faults to a change in spreading direction (along the ridge segment between the faults) can cause adjustment fractures

along one transform fault and slow spreading and shearing along the other transform fault [Menard and Atwater, 1968, Figure 4]. The slow spreading within one of the transform faults is believed to be the cause of great ridges and troughs observed along some sections of fracture zones. Such a mechanism appears ideally suited for resolving both the extreme and linear relief and local tensional character of Canton Trough structures. A similar mechanism has been invoked by Van Andel et al. [1969] to explain the origin for the Vema Fracture in the North Atlantic.

The above discussions indicate that the Canton Trough is a westerly segment of the Clipperton fracture zone formed by a reorientation of spreading centers during the Late Cretaceous epoch. This model adequately accounts for topographic expression, relief, linearity, and trend, and most structure observed throughout the Canton Trough region. However, the occurrence of several samples of fresh volcanic glass and cinder is evidence of volcanism considerably more recent than the Cretaceous. Also, the occurrence of relatively fresh intrusive rocks and several instances of faulted sediments indicates that some faulting has probably occurred well after the formation of the crust in this region. These observations at least necessitate a modification of the original model; namely, rejuvenation of the Canton Trough. A mechanism is therefore needed whereby a portion of an old fracture zone could be tectonically reactivated. Although rejuvenation mechanisms could be presented at this

time, they are unwarranted in light of present knowledge of the region.

Observed magnetic lineations are not easily reconciled with the above model since they trend E-NE rather than perpendicular to the structure. To be made compatible with the reorientation model, extremely linear, regularly-spaced intrusions must be postulated as the magnetic source bodies. These sources must be allowed to cross structural boundaries and transcend the topography. Alternatively, if the magnetic signature predates the formation of the Canton Trough then the anomalies may be attributed to sea-floor spreading phenomena, and the above model is made untenable. It is hoped future work will resolve this dilemma since it is critical to understanding the tectonic processes responsible for the formation of the Canton Trough and its surrounding structures. Similarly, the origin of the plutonic rocks of intermediate composition must be formly established. If it can be determined that they are indigenous and form a sizable intrusive body, their existence on oceanic crust of near-normal thickness must be a foremost consideration in any proposed mechanism of formation.

CONCLUSIONS

The Canton Trough is an elongate, flat-floored deep, flanked by steep en échelon ridges. These features, structurally termed the central province, form a narrow band that is remarkably linear throughout its known length of 500 kilometers. Within this band, maximum recorded trough depths slightly exceed 8000 m, while minimum ridge depths approach 2800 m, and ridge slopes locally are as great at 28°. Rocks recovered from a depth of 7100 m, near the base of the southern ridge, include intermediate- to basic-intrusive rocks, altered fine-grained basalts, fresh, black glass bubbles, and fresh cinder. Although an erratic origin for the intermediate intrusive rocks cannot be denied, an origin by fractionation of basaltic magma is presently favored. The volcanics may include members of both the oceanic tholeiite and alkalic suites. The fresh glass and cinder indicate volcanism considerably more recent than Cretaceous, which is the probable age of the oceanic crust in the region.

The northern structural province, extending at least 100 km north of the Canton Trough, is characterized by block faulting. A relatively large graben within this province forms a structural basin for turbidite deposition presumably from the Line Islands Ridge. The region south of the central province, termed the southern province, is characterized by

a single upfaulted block bordering a wide, undeformed basin containing some turbidites. Toward the Phoenix Islands, this province is characterized by seamounts.

In addition to turbidites acoustically correlated with the stratified unit, radiolarian oozes can be correlated with "transparent" layers. From their apparent stratigraphic positions and general distribution, the deposition of "transparent" sediments is believed to be largely controlled by bottom currents.

Gravity studies indicate nearly normal oceanic crustal thicknesses. However, the depth to the Moho may systematically vary from the eastern to western ends of the surveyed region and the central province is generally characterized by thicker crust than that in adjacent provinces. This may reflect a mass deficiency associated with the intrusion of intermediate rocks. Preliminary magnetic studies indicate elongate bipole residual anomalies as large as 650 gammas. Although magnetic lineations are partly terrain-controlled, they also appear to cross major structural lineations. The magnetic signatures may be generated by linear intrusions related to the structure or they may predate the structure, implying that they are sea-floor spreading anomalies trending E-NE.

The initial formation of the Canton Trough and its associated structures may have resulted from a reorientation

of spreading centers at the East Pacific Rise during the Cretaceous epoch. This mechanism would allow the Canton Trough to be genetically related to the Clipperton fracture zone. However, the mechanism must be modified to allow for rejuvenation of this segment of the Clipperton fracture zone, with consequent volcanism and faulting.

REFERENCES

Aumento, F., Diorites from the Mid-Atlantic Ridge at 45°N, Science, 165, 1112-1113, 1969.

Aumento, F. and B. D. Loncarevic, The Mid-Atlantic Ridge near 45°N-III, Bald Mountain, Can. J. Earth Sci., 6, 11-23, 1969.

Borg, I. Y. and D. K. Smith, Calculated X-ray powder patterns for silicate minerals, Geol. Soc. Amer. Memoir 122, 896 pp., 1969.

Bullard, E. C. and R. I. B. Cooper, Determination of the masses required to produce a given gravitational field, Royal Soc. Proc., Ser. A, 194, 332-347, 1948.

Burnett, W. C., Trace Element Variations in Some Central Pacific and Hawaiian Sediments, Haw. Inst. Geophys. Rept. 71-6 (M.S. Thesis), 112 pp., 1971.

Chase, T. E., H. W. Menard and J. Mammerickx, Bathymetry of the North Pacific, Scripps Institution of Oceanography, 1970.

Emery, K. O., Organic transportation of marine sediments, in The Sea, Volume 3, M. N. Hill, Ed., Interscience, New York, 776-793, 1963.

Engel, A. E. J. and C. G. Engel, Igneous rocks of the East Pacific Rise, Science, 146, 477-485, 1964.

Engel, A. E. J. and C. G. Engel, Igneous rocks of the Indian Ocean Floor, Science, 150, 605-609, 1965.

Engel, A. E. J. and C. G. Engel, Mafic and ultramafic rocks, in The Sea, Volume 4, Part I, M. N. Hill, Ed., Wiley-Interscience, New York, 465-519, 1970.

Engel, A. E. J., C. G. Engel and R. G. Havens, Chemical characteristics of oceanic basalts and the upper mantle, Bull. Geol. Soc. Amer., 76, 719-734, 1965.

Ewing, J. and M. Ewing, Seismic reflection, in The Sea, Volume 4, Part I, M. N. Hill, Ed., Wiley-Interscience, New York, 1-51, 1970.

Ewing, J., M. Ewing, T. Aitken and W. J. Ludwig, North Pacific sediment layers measured by seismic profiling, Geophys. Mono. 12, 147-173, 1968.

Fein, C., Some trace elements in lavas from the Lau Islands, Tofua, Tonga, and Tutuila, American Samoa, Ph.D. Dissertation, University of Hawaii, 97 pp., 1971.

Fox, P. J., E. Schreiber and B. C. Heezen, The geology of the Caribbean crust: Tertiary sediments, granitic and basic rocks from the Aves Ridge, Tectonophysics, 12, 89-109, 1971.

Gast, P. W., Trace element fractionation and the origin of tholeiitic and alkaline magma types, Geochim. Cosmochim. Acta, 32, 1057-1086, 1968.

Halunen, A. J., L. W. Kroenke and B. R. Rosendahl, Geophysical investigation of a deep trough in the Central Pacific (abstract), Trans. Amer. Geophys. Union, 51, 762, 1970.

Hamilton, E. L., Sunken islands of the Mid-Pacific mountains, Geol. Soc. Amer. Memoir 64, 97 pp., 1956.

Harrison, J. C. and W. C. Brisbin, Gravity anomalies off the west coast of North America: Seamount Jasper, Bull. Geol. Soc. Amer., 70, 929-934, 1959.

Hart, S. R. and A. J. Nalwalk, K, Rb, Cs, and Sr relationships in submarine basalts from the Puerto Rico Trench, Geochim. Cosmochim. Acta, 34, 145-155, 1970.

Hayes, D. E. and W. C. Pitman III, Magnetic lineations in the North Pacific, Geol. Soc. Amer. Memoir 126, 291-314, 1970.

Heezen, B. C., B. Glass and H. W. Menard, The Manihiki Plateau, Deep-Sea Res., 13, 445-458, 1966.

Heezen, B. C., E. T. Bunce, J. B. Hersey and M. Tharp, Chain and Romanche fracture zones, Deep-Sea Res., 11, 11-33, 1964.

Hersey, J. B., Continuous reflection profiling, in The Sea, Volume 3, M. N. Hill, Ed., Interscience, New York, 47-71, 1963.

Hubbert, M. K., A line-integral method of computing the gravimetric effects of two-dimensional masses, Geophysics, 13, 215-225, 1948.

Kay, R., N. J. Hubbard and P. W. Gast, Chemical characteristics and origin of oceanic ridge volcanic rocks, J. Geophys. Res., 75, 1585-1613, 1970.

Klug, H. P. and L. E. Alexander, X-ray Diffraction Procedures for Polycrystalline and Amorphous Materials, John Wiley and Sons, Inc., New York - London, 716 pp., 1954.

Krause, D. C., Interpretation of echo sounding profiles, Int. Hydrogr. Rev., 39, 65-123, 1962.

Krause, D. C., H. W. Menard and S. M. Smith, Topography and lithology of the Mendocino Ridge, J. Marine Res., 22, 236-249, 1964.

Kroenke, L. W., Line Islands sediment type, in Woollard, G. P., K. Wyrtki, G. H. Sutton and K. Chave, Annual Progress Report, Contract N00014-70-A-0016-0001, January 1, 1970 - July 31, 1970, Haw. Inst. Geophys. Rept. 70-27, 40-41, 1970.

Kroenke, Loren W., Geology of the Ontong Java Plateau (ms. submitted to Geol. Soc. Amer.).

Kroenke, L. W., R. Moberly, E. L. Winterer and G. R. Heath, Lithologic interpretation of continuous reflection profiling, in Winterer, E. L., and others, Initial Reports of the Deep Sea Drilling Project, Volume VII, Washington, D. C., U. S. Govt. Printing Office, 1161-1226, 1971.

Larson, R. L. and C. G. Chase, Magnetic anomaly lineations and plate tectonics of the Western Pacific in the late Mesozoic (abstract), Trans. Amer. Geophys. Union, 53, 362, 1972.

Macdonald, G. A. and T. Katsura, Chemical composition of Hawaiian lavas, J. Petrol., 5, Part I, 82-133, 1964.

Malahoff, A. and G. P. Woollard, Geophysical studies of the Hawaiian Ridge and Murray Fracture Zone, in The Sea, Volume 4, Part II, M. N. Hill, Ed., Wiley-Interscience, New York, 73-131, 1970.

Malahoff, Alexander, W. E. Strange and G. P. Woollard, Molokai Fracture Zone: Continuation west of the Hawaiian Ridge, Science, 153, 521-522, 1966.

Menard, H. W., Marine Geology of the Pacific, McGraw-Hill, New York, 271 pp., 1964.

Menard, H. W., Extension of Northeastern-Pacific fracture zones, Science, 155, 72-74, 1967.

Menard, H. W. and T. Atwater, Changes in direction of sea floor spreading, Nature, 219, 463-467, 1968.

Menard, H. W. and T. E. Chase, Fracture zones, in The Sea, Volume 4, Part I, M. N. Hill, Ed., Wiley-Interscience, New York, 421-443, 1970.

Miyashiro, A., F. Shido and M. Ewing, Crystallization and differentiation in abyssal tholeiites and gabbros from mid-ocean ridges, Earth Planet. Sci. Letters, 7, 361-365, 1969a.

Miyashiro, A., F. Shido and M. Ewing, Diversity and origin of abyssal tholeiite from the Mid-Atlantic Ridge near 24° and 30° north latitude, Contrib. Mineral. Petrol., 23, 38-52, 1969b.

Moore, D. G., Reflection profiling studies of the California Continental Borderland: Structure and Quaternary turbidite basins, Geol. Soc. Amer. Spec. Paper 107, 142 pp., 1969.

Mueller, G., Methods in Sedimentary Petrology, Hafner Publishing Co., New York - London, 283 pp., 1967.

Nettleton, L. L., Geophysical Prospecting for Oil, McGraw-Hill, New York, 444 pp., 1940.

Philpotts, J. A., C. C. Schnetzler and S. R. Hart, Submarine basalts: Some K, Rb, Sr, Ba, rare earth, H_2O and CO_2 data bearing on their alteration, modification by plagioclase, and possible source materials, Earth Planet. Sci. Letters, 7, 293-299, 1969.

Rosendahl, Bruce R. and A. John Halunen, The petrology and structure of the Canton Trough (abstract), in Geol. Soc. Amer. Abstrs. with Programs, 3, 689, 1971.

Shurbet, G. L., J. L. Worzel and M. Ewing, Gravity measurements in the Virgin Islands, Bull. Geol. Soc. Amer., 67, 1529-1536, 1956.

Smith, J. V., Ed., X-ray powder data file, Sets 1-5, ASTM Special Technical Publication 48-J, 685 pp., 1960.

Smith, J. V., Ed., Index to the powder diffraction file, ASTM Special Technical Publication 48-N2, 786 pp., 1964.

Sutton, G. H., G. L. Maynard and D. M. Hussong, The widespread occurrence of the 7.4-7.6 km/sec basal crustal layer in the Pacific Ocean Basin, in Woollard, G. P., K. Wyrtki, G. H. Sutton and K. Chave, Annual Progress Report, Contract N00014-70-A-0016-0001, January 1, 1970 - July 31, 1970, Haw. Inst. Geophys. Rept. 70-27, 53-64, 1970.

Talwani, M., J. L. Worzel and M. Landisman, Rapid gravity computations for two-dimensional bodies with application to the Mendocino submarine Fracture Zone, J. Geophys. Res., 64, 49-59, 1959a.

Talwani, M., G. H. Sutton and J. L. Worzel, Crustal section across the Puerto Rico Trench, J. Geophys. Res., 64, 1545-1555, 1959b.

Tatsumoto, M., C. E. Hedge and A. E. J. Engel, Potassium, rubidium, strontium, thorium, uranium, and the rate of strontium-87 to strontium-86 in oceanic tholeiitic basalt, Science, 150, 886-888, 1965.

Van Andel, T. H., J. D. Phillips and R. P. Von Herzen, Rifting origin for the Vema Fracture in the North Atlantic, Earth Planet. Sci. Letters, 5, 296-300, 1969.

Vening-Meinesz, F. A., J. H. V. Umbgrove and Ph. H. Kuenen, Gravity Expedition at Sea, 1923-1932, Volume 2, Pub. Netherl. Geod. Comm., 208 pp., 1934.

Wilson, J. T., A new class of faults and their bearing on continental drift, Nature, 207, 343-347, 1965.

Winterer, E. L. and others, Initial reports of the Deep Sea Drilling Project, Volume VII, Washington, D. C., U. S. Govt. Printing Office, 1971.